Massachusetts Institute of Technology
Department of Civil Engineering
Constructed Facilities Division
Cambridge, Massachusetts 02139

FLEXIBLE SUB-SURFACE BUILDING-FOUNDATION INTERFACES FOR ASEISMIC DESIGN

Preliminary Studies

by

Evelyn Raupach
Betsy Schumacker
John M. Biggs

April 1981

Sponsored by the National Science Foundation
Division of Problem-Focused Research
Grant PFR 79-02989

Publication No. R81-8 Order No. 695

0272-101

REPORT DOCUMENTATION PAGE	1. REPORT NO. NSF/CEE-81020	2.	3. Recipient's Accession No. PB81 243891
4. Title and Subtitle Flexible Sub-Surface Building-Foundation Interfaces for Aseismic Design (Preliminary Studies)			5. Report Date April 1981
			6.
7. Author(s) E. Raupach, B. Schumacker, J.M. Biggs			8. Performing Organization Rept. No. R81-8
9. Performing Organization Name and Address Massachusetts Institute of Technology Department of Civil Engineering Constructed Facilities Division Cambridge, MA 02139			10. Project/Task/Work Unit No. No. 695 11. Contract(C) or Grant(G) No. (C) (G) PFR7902989
12. Sponsoring Organization Name and Address Directorate for Engineering (ENG) National Science Foundation 1800 G Street, N.W. Washington, D.C. 20550			13. Type of Report & Period Covered
			14.

15. Supplementary Notes

Submitted by: Communications Program (OPRM)
National Science Foundation
Washington, D.C. 20550

16. Abstract (Limit: 200 words)

The feasibility of constructing buildings on horizontally flexible foundations to mitigate the effects of earthquakes is explored. The specific concept studied involves the use of slender steel piles enclosed in sleeves to permit flexural distortion. Piles are designed by a simple procedure using smoothed response spectra. The performance of the designed systems are then studied using time histories of actual ground motions. It is shown that the simple design procedure is adequate. Building-pile systems with periods up to 12 seconds are found to be physically feasible. This results in maximum building forces corresponding to seismic coefficients less than current code requirements even though the building remains elastic. The report includes descriptions of ground motions used in the study, pile design equations and procedures, and the time-history analysis.

17. Document Analysis a. Descriptors

Earthquakes	Structural dynamics	Foundations
Earthquake resistant structures	Structural engineering	Feasibility
Design criteria	Dynamic response	Pile structures

b. Identifiers/Open-Ended Terms

Ground motion

c. COSATI Field/Group

18. Availability Statement	19. Security Class (This Report)	21. No. of Pages
NTIS	20. Security Class (This Page)	22. Price

(See ANSI-Z39.18) See Instructions on Reverse

OPTIONAL FORM 272 (4-77)
(Formerly NTIS-35)
Department of Commerce

ABSTRACT

Reported herein is an investigation of the feasibility of constructing buildings on horizontally flexible foundations to mitigate the effects of earthquakes. The specific concept studied involves the use of slender steel piles enclosed in sleeves to permit flexural distortion.

Piles are designed by a simple procedure using smoothed response spectra. The performance of the designed systems are then studied using time histories of actual ground motions. It is shown that the simple design procedure is adequate.

Building-pile systems with periods up to 12 seconds are found to be physically feasible. This results in maximum building forces corresponding to seismic coefficients less than current code requirements even though the building remains elastic. The economic feasibility of the concept has not yet been studied.

ACKNOWLEDGEMENTS

This is the third report issued under the research project entitled "Flexible Sub-surface Building-Foundation Interfaces for Aseismic Design." The project is supported by the National Science Foundation, Division of Problem-Focused Research Applications, under Grant PFR-7902989. The previous reports (References 6 and 7) provided information on pile-soil interaction and on ground motion which was used in the study reported here.

Dr. John B. Scalzi is the cognizant NSF program official, and his support is gratefully acknowledged. Professor Emeritus Myle J. Holley, Jr. of MIT provided valuable assistance and advice as an unpaid consultant.

The opinions, findings and conclusions or recommendations expressed in this report are those of the authors and do not necessarily reflect the views of the National Science Foundation.

TABLE OF CONTENTS

CHAPTER I - INTRODUCTION

The purpose of the research project under which this report has been produced is to investigate the effectiveness and feasibility of constructing buildings on horizontally flexible foundations to mitigate the effects of earthquakes. If successful, the concept would permit the design of the building for very modest lateral forces and yet limit the earthquake response to essentially elastic behavior. Thus far, these studies have been limited to the sleeved-pile system, in which flexibility is achieved by the bending of slender steel piles within a sleeve (or caisson) below grade.

Reported herein are certain preliminary studies based upon simple models for both analysis and design. Cylindrical steel piles are designed for various values of the significant parameters and for responses predicted by smoothed spectra. The building-pile systems are then subjected to real ground motions to verify the designs and to determine the response in more detail.

1.1 Background

Much of the past and current research in earthquake engineering was and is directed toward improvements in the analysis and design of conventional systems (e.g., building frames). Most of these systems were developed without regard to seismic requirements. There is therefore an obvious need for the development of new systems which will more effectively and economically provide earthquake protection.

The general concept of increasing the structure's flexibility, and hence lengthening the natural period, is well understood. This has the effect of reducing the inertia forces on the structure and therefore the required strength. There is, however, a corresponding increase in horizontal displacements which must be accommodated.

The design of conventional buildings under current codes is based on relatively small equivalent static loads and anticipates considerable yielding and hence serious damage in a severe earthquake. If a flexible interface concept, can only be aggravated when the effects of vertical components of earthquake motion are introduced.

Another concept which has been investigated involves the use of flexible rubber bearings at the foundation together with energy-absorbing devices to increase damping (Refs. 4 & 5). For the systems studied there was only a modest increase in the period of the fundamental mode. Although the seismic inertia force was considerably decreased, much of this was due to increased damping rather than decreased stiffness.

In the concept investigated here, the desired elastic flexibility is introduced below grade as part of the foundation, thus eliminating some of the disadvantages cited above. The system provides isolation by a substantial increase in natural period with a high degree of reliability.

1.2 The Sleeved-Pile Concept

Basically, the concept studied herein involves the insertion of a soft spring between the building superstructure and the soil foundation. Various implementation schemes can be envisaged. However, the vehicle for this study is a system utilizing sleeved piles which, through flexure, provide the desired spring action. The analytical results obtained are valid for any soft spring system, but it is believed desirable that the study be done in relation to at least one practicable means of implementation.

The sleeved pile is comprised of a pile with a sleeve of substantially larger diameter, arranged to permit large bending moments in the pile without excessive soil stresses and strains (see Fig. 1.1). The principal function of the sleeve is to provide a pile "free length," thereby achieving flexible, low-stiffness response to horizontal loading at the pile top. Secondly, the sleeve permits transfer of horizontal reactions from pile to soil well below the ground surface: that is, at depths where the soil resistance to such lateral forces is great. For the present purpose, it is sufficient to note that the sleeve concept permits the design of a pile not only to support large vertical loading, but, in addition, to accept large lateral displacements at its upper end.

The length of unconfined portions of the pile (i.e., within the embedded sleeve plus any portion projecting above the embedment) and the pile cross section may be chosen to satisfy lateral strength and stiffness requirements. The pile may be supported by a concrete infill, as shown in Fig. 1.1, or by pile-to-sleeve connections at discrete elevations. For purposes of this study the pile will be treated as "fixed" by a concrete infill as shown in Fig. 1.1.

For a building supported on sleeved piles we may visualize the piles as providing a horizontal shear spring of predictable, elastic, stiffness. Because this force-displacement relationship is not associated with friction, or with large distortions of a nonlinear material, but rather with flexural distortion of the piles, it is not only predictable, but can be age-independent. The fundamental period of the total system may be made very long, perhaps as long as 20 seconds, although this may not be the optimum solution.

In summary, it is believed that the sleeved-pile concept has several advantages over the above-grade soft story concept. These include:

1. A greater length is available to achieve the desired flexibility and any desired natural period could be achieved.

2. Because only elastic behavior is involved, the properties of the system can be accurately predicted.

3. Although seismic stresses in the pile would be high, safety against collapse (due to larger than design earthquake motions and/or the P-Δ effect) is ensured because the ground provides a limit to horizontal displacement. Under gravity loads alone, the axial pile stress is small and, with the pile restrained at its top by a wind-resisting device, the factor of safety is large.

4. It should be easier to accommodate the necessarily large deflections at ground level than in the bottom story of the superstructure.

5. It would be possible to build damping devices into the system at the piles and thus achieve an optimum value. Much higher damping than normally found in structures would be beneficial and possibly economically feasible.

In Chapter V the results are summarized and conslusions are drawn from these preliminary studies. No attempt is made to investigate the economic feasibility of the sleeved-pile concept. This will be undertaken in a later phase of the project.

CHAPTER II - GROUND MOTIONS

2.1 Introduction

Most accelerographs record the characteristics of the ground motion induced by earthquakes by means of a stiff, highly damped, linear time-invariant and single-degree-of-freedom transducer. The relative displacement response of this transducer is proportional to the acceleration of the ground motion. Thus, it is theoretically relatively straightforward to recover the ground motion from the transducer response. However, the transducer response is an analog signal and for engineering use it is desirable to use a digital signal of the ground motion. The ground acceleration, then, undergoes several transformations before being available as a digital signal, and associated with each of these transformations are several sources of errors which affect the reliability of the signal. Processing procedures in the form of computer programs were developed (originally by Trifunac and Lee, Ref. 11) in order to minimize the presence of errors or noise in the ground motion signals. These procedures were based on the state of the art of signal processing in the late nineteen sixties, and these procedures have been used to process (or correct) all digitized strong-motion records in this country. In particular, all the records available from Cal Tech and known as the Cal Tech records were processed using these procedures.

The most critical phase of the processing is the phase that goes (in Cal Tech terminology) from Volume I uncorrected records to Volume II corrected records. This phase performs instrument correction, band-pass filtering, and integration. It is called the most critical since it is the output from this phase that is used in engineering applications and, in particular, is needed for use in this study.

The state of the art of digital signal processing has changed tremendously since the 1960's (or since the implementation of the original processing procedures), and thus it is now possible to develop a new processing procedure incorporating up-to-date signal-processing techniques which would remove most of the deficiencies inherent in the original processing scheme. These deficiencies are primarily the following:

Step 5. Integrate the acceleration using the Schuessler-Ibler integration rule to obtain the velocity signal. Assume zero initial velocity.

Step 6. Integrate the velocity using the Schuessler-Ibler integration rule to obtain the displacement signal. Assume zero initial displacement.

This processing scheme exists as a computer software package and was used to process the records which are used in this study. The records so chosen are described next. The theory, methodology, and details for the new processing procedure are described in an earlier project report, namely, "On the Standard Processing of Strong-Motion Earthquake Signals," by Shyam Sunder (7).

2.3 Records Used in Study

For the purposes of this study it was desirable to locate strong-motion records which could be processed with filter limits that would provide frequency content down to at least 0.1 hz (or out to at least 10 seconds). Toward this end, all Cal Tech strong-motion records and all records available from the Environmental Data Service, NOAA, in Boulder were examined. Most of these records were reliable only out to about 2 to 6 seconds. However, four horizontal-vertical motion pairs were found which could be filtered out to at least 12 seconds. These seven records, which are the ones used in this study, are summarized in Table 2.1. The two Long Beach motions form one pair, the two Sitka form another pair, the Imperial Valley 230 and Up form a third pair, and the Imperial Valley 140 and Up form the fourth pair. Table 2.2 summarizes the peak acceleration, velocity, and displacement for each of these records, as well as the times at which the peaks occur. The acceleration and displacement time histories for each of these records are plotted in Fig. A.1 through A.14.

Single-degree-of-freedom oscillator responses to each of the corrected strong-motion records were computed for four damping values (0, 2 1/2, 5 and 10%), and 24 periods (.01, .02, .03, .05, .067, .1, .25, .5, 1, 1.5, 2, 2.5, 3, 4, 5, 6, 7, 8, 9, 10, 12, 14, 16, and 18 seconds). The spectral accelerations and spectral displacements for 0% and 10% damping

	Acceleration		Velocity		Displacement	
Reference ID	cm/sec^2	Time	cm/sec	Time	cm	Time
EQ-3 (H)	226.64	10.99	28.60	14.70	-21.48	13.87
EQ-3 (V)	-371.04	11.35	32.34	9.73	23.42	11.41
EQ-4 (H)	76.37	16.58	-10.67	23.58	-10.07	25.30
EQ-4 (V)	-47.74	15.98	- 4.47	23.09	- 2.56	24.11
EQ-1 (H)	451.78	13.12	111.48	14.06	46.77	14.98
EQ-1 (V) EQ-2 (V)	-586.62	11.01	26.77	10.91	9.48	15.35
EQ-2 (H)	331.78	14.63	49.88	16.01	25.99	17.00

Table 2.2 Peak Acceleration, Velocity and Displacement

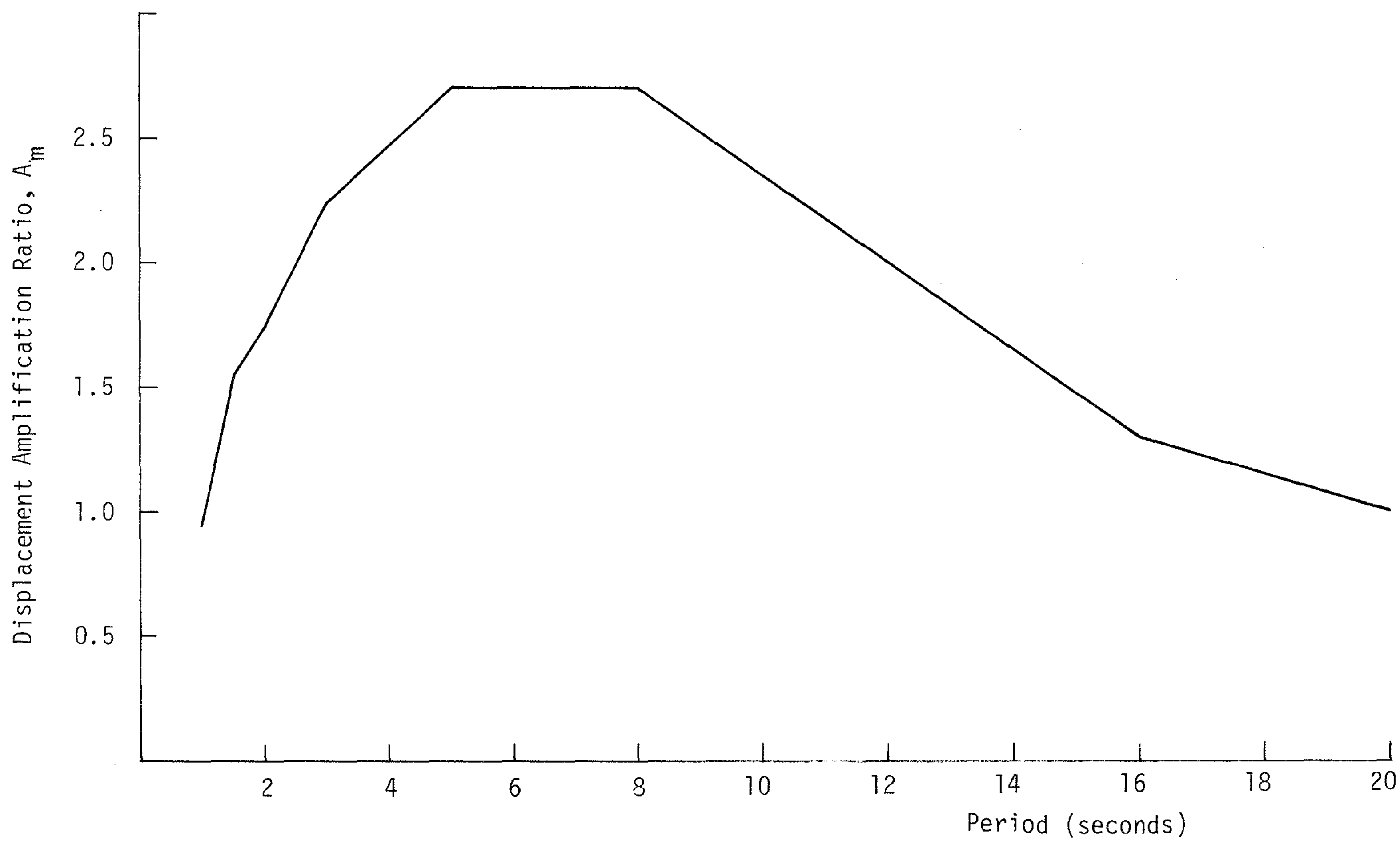

Fig. 2.1 Horizontal Displacement Design Spectrum
0% Damping

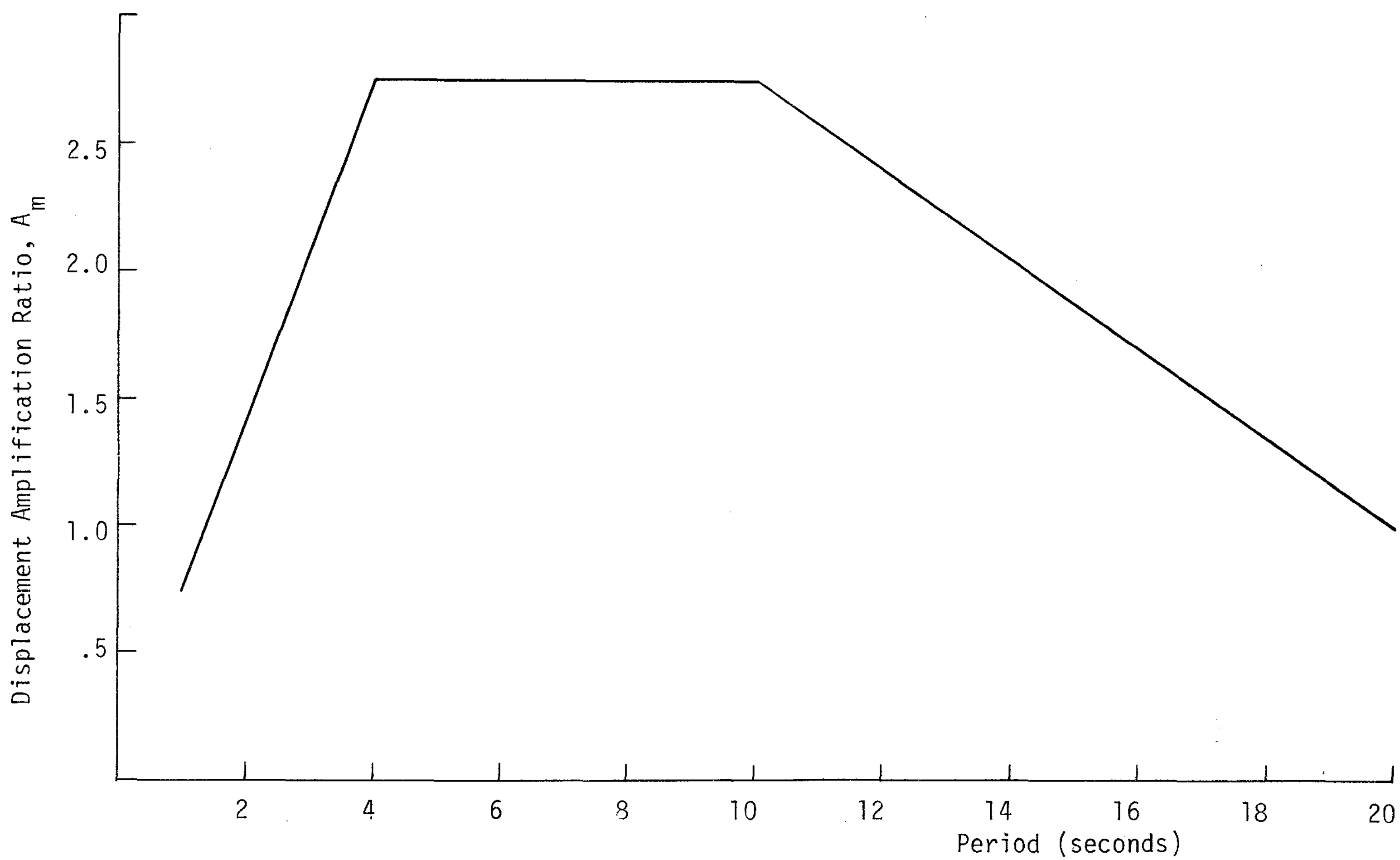

Fig. 2.3 Vertical Displacement Design Spectrum

0% Damping

CHAPTER III - DESIGN OF PILES

3.1 Introduction

The objective of this chapter is to develop a simple design procedure for the pile of the sleeved-pile system. The sleeved pile is comprised of a pile within a sleeve of substantially larger diameter where for the purpose of this study the pile will be treated as "fixed" by a concrete infill, as in Fig. 1.1. In the present study the design of the sleeve is not considered, since its diameter and thickness are not of critical importance. The design is developed for a single pile in an infinite halfspace; the effect of "grouping" of piles and of overturning moment will be investigated in a later report.

Depending upon specific site conditions and upon design choices, a variety of degrees of fixity at top and bottom of the pile free length may be realized. For the purposes of this study two extreme conditions are evaluated: (1) fully-fixed at bottom and ideally pinned at top, and (2) fully-fixed top and bottom. Included in this chapter are the design equations and procedures for three types of piles (all are of constant tube wall thickness):

(1) constant diameter piles, fixed at the bottom and hinged at the top;

(2) constant diameter piles, fixed at the top and bottom; and

(3) tapered piles, fixed at the bottom and hinged at the top.

Descriptions of the three pile types are presented in the following sections.

Several pile designs are summarized in plots presented in Section 3.4. The plots show the resulting pile design length and diameter and the corresponding ratio of the pile axial load to the Euler buckling load, P/P_E, as functions of the pile type and the pile design parameters: design period; pile damping ratio; pile axial load; pile wall thickness; and design steel stress.

To obtain this simple one-degree model the horizontal and rotational soil stiffnesses are approximated at infinity (i.e., the soil flexibility is ignored). The building superstructure is assumed rigid and its rotational inertia is ignored. In this preliminary pile design the effect of vertical ground motion will be ignored.

Kaynia (6) developed equivalent stiffness expressions for the pile in the horizontal direction for pile types (1) and (2). Imposing the assumptions stated, these expressions simplify as follows: If ℓ and EI are the free length and bending rigidity of the pile, the equivalent stiffness of this member in the horizontal direction is given by

type (1)

$$k_p = \frac{3EI}{\ell^3} \frac{a^3}{3} \frac{1}{\tan a - a} \tag{3.1}$$

type (2)

$$k_p = \frac{12EI}{\ell^3} \frac{a^3}{12} \frac{\sin a}{2 - 2 \cos a - a \sin a} , \tag{3.2}$$

where the dimensionless parameter a is defined as

$$a = \sqrt{\frac{P\ell^2}{EI}} , \tag{3.3}$$

and P is the axial force in the pile, $P = M_t g$, where the total mass, M_t, is the sum of the building and foundation masses. If EI_0 is the bending rigidity of the tapered pile at its base, the equivalent horizontal stiffness for pile type (3) is approximately given by

type (3)

$$k_p = \frac{27}{11} \frac{EI_0}{3} \frac{a^3}{3} \frac{1}{\tan a - a} , \tag{3.4}$$

where a is defined as $\sqrt{P\ell^2/EI_0}$. The underlying analytical assumptions are discussed in Section 3.3.3.

The pile is designed to develop the maximum displacement and shear obtained from the smoothed design spectrum (presented in Chapter II)

3.3 Pile Design Equations

The pile designs are presented as a function of the desired fundamental period of the final system, which is very near the period of the one-degree simplified model. The other variables considered are the axial load in the pile (which can be varied by adjusting the pile spacing), the thickness of the pile wall, the yield stress of the steel, and the damping between the foundation and the ground provided by the pile itself or by a damping device added for this purpose. For given values of these parameters the pile length and diameter are determined.

3.3.1 Constant Diameter Piles Hinged at Top

The pile length is obtained from the equivalent horizontal stiffness expression. Dividing Eq. (3.1) through by the Euler buckling load for a column hinged at the top and fixed at the base, and noting that the frequency is defined as

$$\omega_p = \sqrt{\frac{k_p}{M_t}} = \sqrt{\frac{k_p}{P/g}} \ , \tag{3.7}$$

we arrive at the expression

$$\frac{k_p}{P_E} = \frac{\omega_p^2}{g} \left(\frac{P}{P_E}\right) = \frac{12}{\pi^2 \ell} \frac{a^3}{3} \frac{1}{\tan a - a} \ , \tag{3.8}$$

where the dimensionless parameter a is now defined as

$$a = \frac{\pi}{2} \sqrt{\frac{P}{P_E}} \ . \tag{3.9}$$

Solving Eq. (3.9) for the pile length, the final expression is

$$\ell = \frac{4g}{\omega_p^2 \pi^2 \left(\frac{P}{P_E}\right)} a^3 \frac{1}{\tan a - a} \ . \tag{3.10}$$

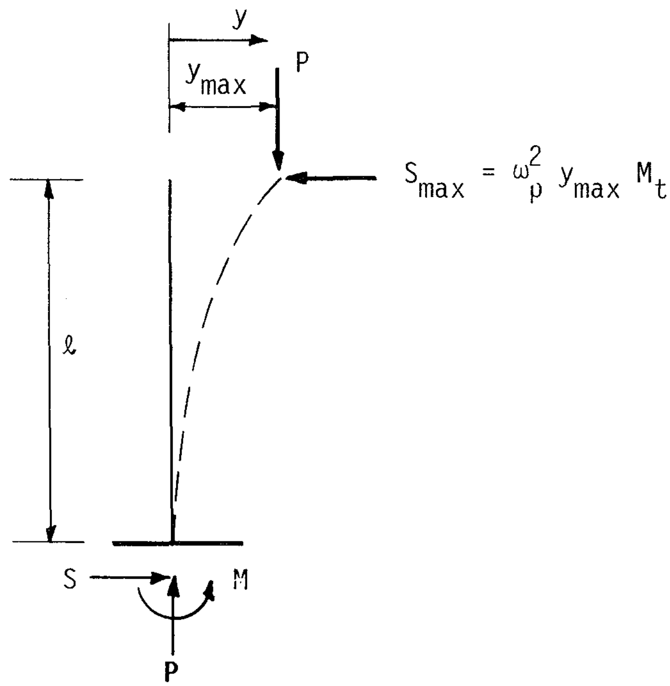

Fig. 3.2 Equilibrium of Displaced Pile

3.3.2 Constant Diameter Piles Fixed at the Top

Proceeding in a similar manner as in Section 3.3.1, Eq. (3.2) can be used to derive an expression for the pile length

$$\ell = \frac{g}{\omega_p^2 \, \pi^2 \, (\frac{P}{P_E})} \, a^3 \, \frac{\sin a}{2 - 2 \cos a - a \sin a} \, , \tag{3.17}$$

where the dimensionless parameter a is now defined as

$$a = \pi \sqrt{\frac{P}{P_E}} \, , \tag{3.18}$$

note the Euler buckling load for a column fixed against rotation at both top and bottom and free to displace at the top is given by

$$P_E = \frac{\pi^2 EI}{\ell^2} \, . \tag{3.19}$$

case of tapered piles hinged at the top. The only difference is that the tapered pile stiffness and Euler buckling load differ from those of pile type (1) by a constant.

The Euler buckling load is approximated by

$$P_E = 1.958 \frac{EI_o}{\ell^2} \quad , \tag{3.22}$$

where EI_o is the bending rigidity at the base of the tapered pile.

The pile length expression obtained from the stiffness Eq. (3.4) is given by

$$\ell = \frac{1.254\ g}{\omega_p^2 \ (\frac{P}{P_E})} \ \frac{a^3}{3} \ \frac{1}{\tan a - a} \quad , \tag{3.23}$$

where the parameter a is defined as

$$a = \frac{\pi}{2} \sqrt{\frac{P}{P_E}} \quad . \tag{3.24}$$

The moment of inertia at the base of the tapered pile is computed from Eq. (3.22) and given by

$$I_o = \frac{P\ell^2}{1.958\ E\ (\frac{P}{P_E})} \quad . \tag{3.25}$$

The pile stress and thickness equations are identical to (3.15) and (3.16) respectively.

3.4 Pile Design Procedure

For the purpose of the present study a pile design procedure, applicable to all three pile types, was developed. The scheme is outlined below.

3.5 Comments on Pile Designs

In this section an array of pile designs is shown in the form of plots of length and diameter versus period. The effects of the design parameters, pile damping ratio, steel yield stress, pile axial load, and thickness are also discussed. The various combinations of design parameters included in the present study are tabulated in Table 3.1. The values of these parameters, selected for illustration, represent readily available materials, (i.e., 414 and 689 MPa (60 and 100 ksi)) steel yield strengths, 2.54 and 3.81 cm (1 and 1.5 inch) pile wall thicknesses). The pile axial loads (P) reflect reasonable pile spacings under buildings of moderate height. These design combinations are repeated for periods of the one-degree model ranging from 6-12 seconds.

All the piles are designed assuming a peak ground displacement of 30.48 cm, which is a reasonable design value (i.e., maximum predicted) for many seismic areas. The designs are based upon the smoothed design spectra presented in Chapter II. The design values of displacement and acceleration are tabulated in Table 3.2. When the pile systems are subjected to time-history analysis, the results (i.e., acceleration of building, pile displacement and stress, etc.) will be scaled in proportion to the spectral displacement of the time-history (earthquake) being used, thus eliminating the effect of earthquake strength. These scaling factors will be discussed and tabulated in Chapter IV.

The feasibility of a specific pile design depends not only on reasonable design values of pile length and diameter, etc., but on the cost of materials, fabrication and construction. Feasibility due to cost considerations are not discussed in the present study, but will be the subject of later investigation.

Figures (3.3) to (3.8) summarize the results of several designs of pile type (1), (constant diameter pile hinged at the top). Plots of pile length, pile diameter and the ratio P/P_E versus the period of the one-degree model are presented. Figures (3.3) to (3.5) and (3.6) to (3.8) correspond to steel design yield stresses of 414 MPa (60 ksi) and 689 MPa (100 ksi), respectively, and a pile damping of 0.5%. Observe that the pile length and diameter decrease approximately 33 and 40 percent as the period of the one-degree model increases from 6 to 12 seconds. The opposite is true for P/P_E, which increases with the period.

	Period of the One-Degree Model						
	6	7	8	9	10	11	12

Pile Damping Ratio 0.5%

Displacement (cm)	82.296	82.296	82.296	77.114	71.628	66.142	60.960
Acceleration (cm/sec^2)	90.248 (0.092g)	66.304 (0.068g)	50.764 (0.052g)	37.585 (0.038g)	28.278 (0.029g)	21.580 (0.022g)	16.713 (0.017g)

Pile Damping Ratio 10%

Displacement (cm)	50.292	49.530	48.768	47.224	45.720	44.196	42.672
Acceleration (cm/sec^2)	55.151 (0.056g)	39.905 (0.041g)	30.082 (0.031g)	23.026 (0.023g)	18.050 (0.018g)	14.420 (0.015g)	11.699 (0.012g)

Table 3.2 Design Displacement and Acceleration for β_p =.5%, 10%.
Peak Ground Displacement = 30.48 cm.

Two pile designs of each of the pile types (1) and (2) are presented in Figs. (3.9) and (3.10). Fixing the pile-top connection results in approximately a 29 percent increase in the pile length and a 23 percent decrease in the pile diameter. These percent decreases or increases are typical of any combination of design parameters.

Figures (3.11) and (3.12) present pile designs of pile types (1) and (3). The tapered pile designs show approximately an 11 percent decrease in pile length and effectively no change in pile diameter over the constant diameter pile. Again these results are typical of all pile design parameter combinations.

The percent decrease or increase in pile length, diameter, and the ratio P/P_E, accompanying an increase in pile damping is dependent on the period of the one-degree model. In the case of the pile length, the percent decrease for 10 percent damping ranges from 33 (6 seconds) to 23 (12 seconds). The percent decrease in pile diameter ranges from 30 (6 seconds) to 17 (12 seconds). The increase in the ratio P/P_E ranges from 20 percent (6 seconds) to 6 percent (12 seconds). The addition of damping devices may be a cost-effective way to decrease pile size.

The advantages of increased period of the pile system, damping and steel yield stress are significant in reducing the pile length. In the present study, values of T_p, β_p, and f_Y of 10 - 12 seconds, 10 percent and 689 MPa respectively, result in the shortest pile lengths (see Fig. (3.6)). Increasing the pile thickness and decreasing the pile axial load also contribute to reductions in pile length. Corresponding to the reduction in pile length is a reduction in pile diameter. As the design period increases, the diameter decreases, and at large periods some of the ratios of pile thickness to diameter shown may not be reasonable. A disadvantage in reducing the pile axial load is the increase in the number of piles necessary to support the same superstructure.

There appears to be no significant advantage in using tapered piles rather than constant diameter piles. The decrease in pile length due to taper is probably outweighed by the increase in fabrication cost. However, the use of tapered piles will result in a somewhat smaller diameter sleeve.

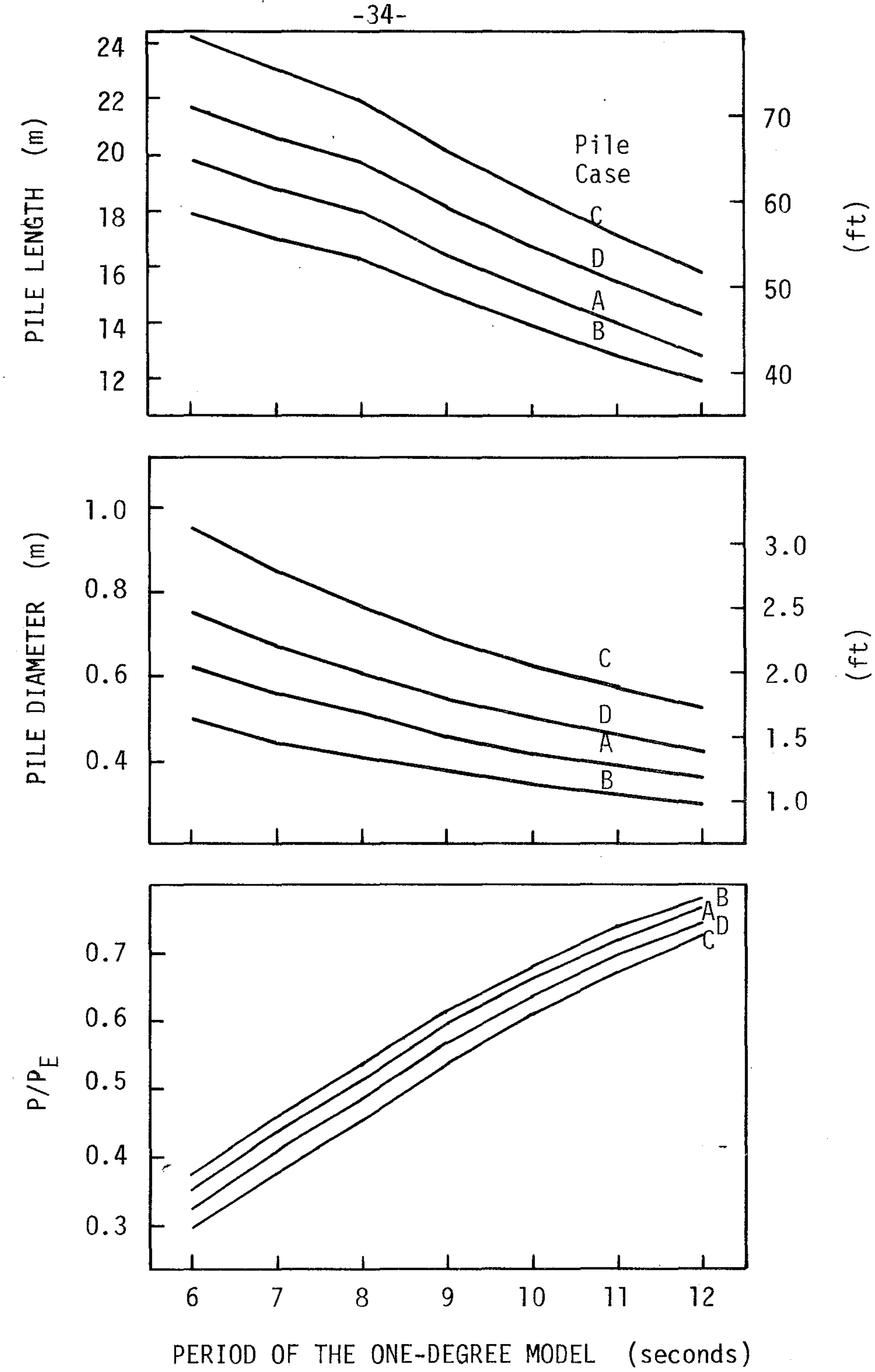

Figs. 3.3, 3.4 & 3.5 Pile Length, Pile Diameter, and Ratio P/P_E for β_p = 0.5%, f_y = 414 MPa (60 ksi)

Pile Type (1) Designs

See Table 3.1 for Pile Case Identification

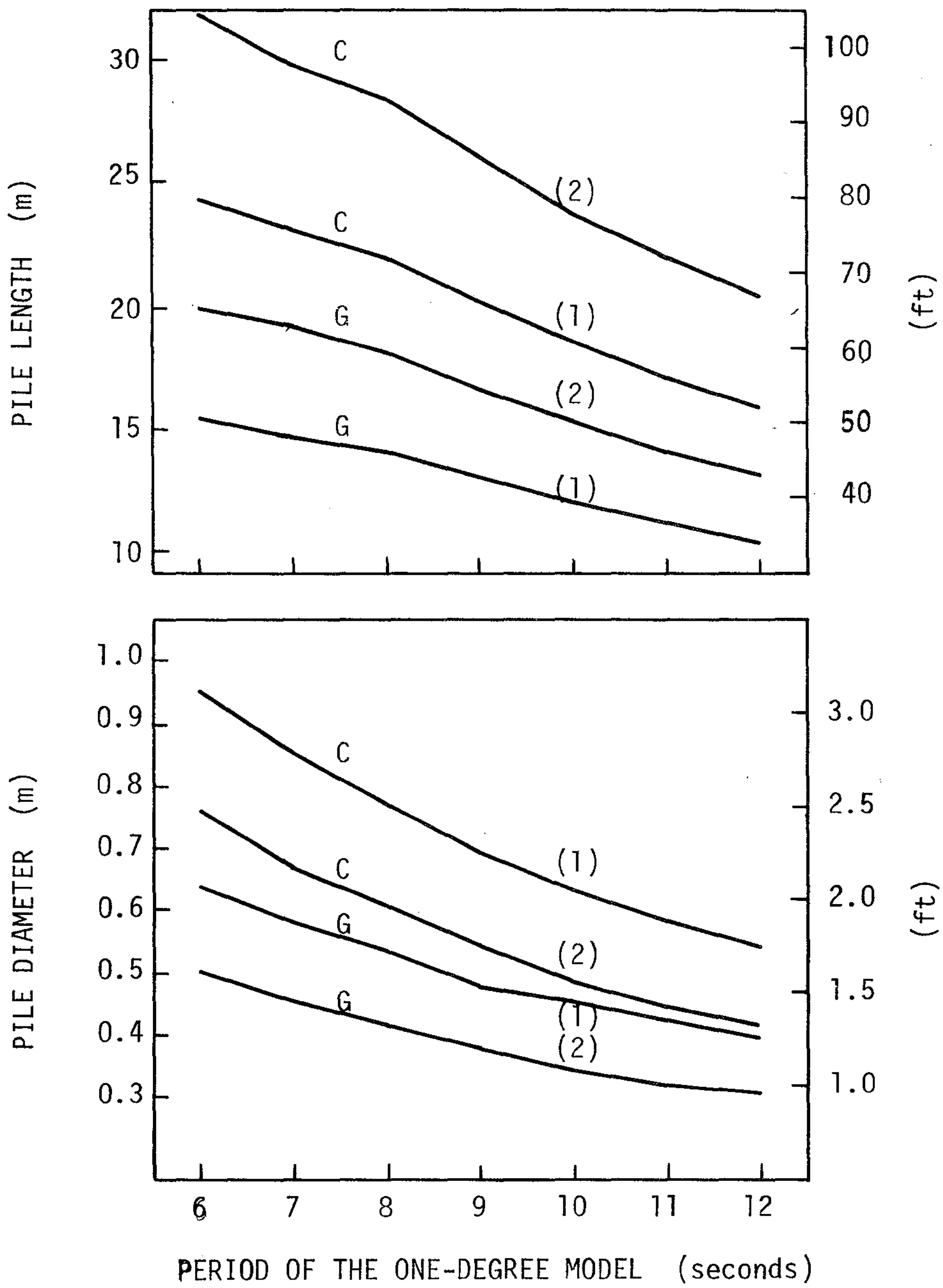

Figs. 3.9 & 3.10 Pile Length and Pile Diameter for β_p = 0.5%. Piles with pinned top (Type 1) and fixed top (Type 2).

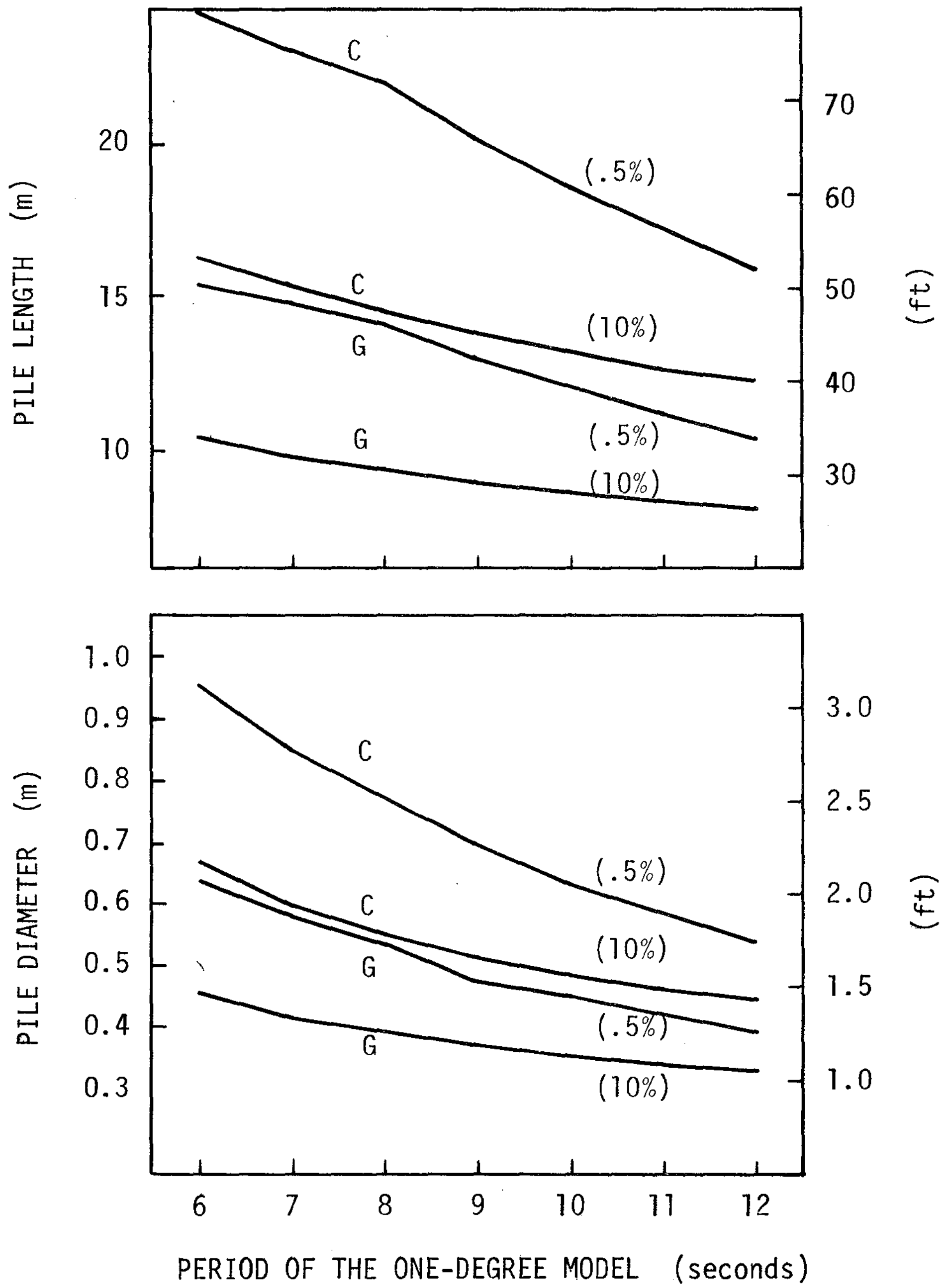

Figs. 3.13 & 3.14 Effect of Pile Damping on Pile Length and Pile Diameter Pile Type (1) Designs

CHAPTER IV - TIME HISTORY ANALYSES

4.1 Introduction

The purpose of this chapter is to verify the simplified pile design procedure based on the single pile, one-degree model developed in Chapter III and to investigate in more detail the response of the systems to real earthquake motions, including the peak forces on the building structure. The one-degree design model is replaced by the three-degree analytic models in Fig. 4.1. Fig. 4.1(a) represents the three-degree model for vertical vibration and 4.1(b) that for horizontal vibration. We investigate only the type (1) pile, which is of constant diameter and hinged at the top. The models simulate the fundamental mode of the building and the flexibility of the soil around the sleeve.

The piles were designed, as described in Chapter III, for the maximum response condition (i.e., the magnitudes of the maximum pile displacement and maximum pile acceleration were obtained from the smoothed design spectra). The motions of the ground during an earthquake are essentially random; i.e., the peaks of acceleration, both positive and negative, have various amplitudes and occur at various time intervals without any regular pattern. Both the magnitude of the input (i.e., acceleration), and its time variation, have an important effect on the structural response. The effects of the details of the ground motion upon the structural response of the three-degree model will be investigated in this chapter. If one refers to the response spectrum for the horizontal earthquakes used in this study, for any particular period of the one-degree model, each earthquake exhibits a different magnitude for the peak spectral displacement response. This is due to the varying strengths of the earthquakes. To negate this effect the results of the time-history analyses of the real earthquake records are scaled so as to cause approximately the same peak response as obtained from the smoothed design spectrum at the period of the system being investigated. The results of the time-history analyses of possible pile designs are presented in tables and plots. Four pairs of vertical and horizontal earthquake ground motions are used.

The effect of vertical vibration on horizontal response of the three-degree model is investigated in Section 4.6. The effect of the building period, the inclusion of a rigid-brittle wind-resisting device into the

List of Symbols Used in Analytical Model

β_b = building damping ratio

β_p = pile damping ratio

c_b = building viscous damping = $\beta_b(2M_b 2\pi/T_b)$

c_p = pile viscous damping = $\beta_p \left\{2(3M_b + M_f)\ 2\pi/T_b)\right\}$

c_{xx} = translational soil viscous damping in the horizontal direction, Eq. (4.11)

c_{zz} = translational soil viscous damping in the vertical direction, Eq. (4.12)

k_b = equivalent building stiffness for given building period = $(2\pi/T_b)^2 M_b$

k_p = horizontal pile stiffness, Eq. (4.17)

k_{pz} = vertical pile stiffness, Eq. (4.19)

k_{xx} = translational soil stiffness in the horizontal direction, Eq. (4.8)

k_{zz} = translational soil stiffness in the vertical direction, Eq. (4.12)

$k_{\phi\phi}$ = rotational soil stiffness, Eq. (4.9)

M_b = equivalent building mass per pile = 1/3 x real mass (assuming the building mass is uniform with height and has a linear mode shape)

M_f = foundation mass per pile

M_p = arbitrary small pile mass

M_t = total real mass = $3M_b + M_f$

T_b = fundamental building period excluding foundation effects

T_p = period for pile with rigid building = $2\pi\sqrt{(3M_b + M_f)/k_p}$

ω_b = fundamental building frequency

ω_p = frequency for pile with rigid building

y_b = relative building displacement

y_f = foundation displacement

y_p = pile displacement

y_s = ground displacement

$\dot{}$ = first derivative with respect to time

$\ddot{}$ = second derivative with respect to time

Introducing convenient parameter ratios, simplifying, and rewriting in matrix notation, the final expressions become

$$\begin{vmatrix} R_2 & \frac{3}{2}R_2 & 0 \\ \frac{3}{2}R_2 & 1 & 0 \\ 0 & 0 & R_4 \end{vmatrix} \begin{vmatrix} \ddot{y}_b \\ \ddot{y}_f \\ \ddot{y}_p \end{vmatrix} + \begin{vmatrix} 2\beta_b\omega_b R_2 & 0 & 0 \\ -2\beta_b\omega_b R_2 & 2\beta_p\omega_b R_1 & -2\beta_p\omega_b R_1 \\ 0 & -2\beta_p\omega_b R_1 & 2\beta_p\omega_b R_1 + \omega_b^2 R_1^2 R_3 R_5 \end{vmatrix}$$

$$\begin{vmatrix} \dot{y}_b \\ \dot{y}_f \\ \dot{y}_p \end{vmatrix} + \begin{vmatrix} \omega_b^2 R_2 & 0 & 0 \\ 0 & \omega_b^2 R_1^2 & -\omega_b^2 R_1^2 \\ 0 & -\omega_b^2 R_1^2 & \omega_b^2 R_1^2 (1 + R_3) \end{vmatrix} \begin{vmatrix} y_b \\ y_f \\ y_p \end{vmatrix}$$

$$= \begin{vmatrix} 0 \\ 0 \\ \omega_b^2 R_1^2 R_3 R_5 \dot{y}_s + \omega_b^2 R_1^2 R_3 y_s \end{vmatrix}, \tag{4.4}$$

where the parameters R_1 through R_5 are defined as

$R_1 = \dfrac{\omega_p}{\omega_b}$, ratio of pile to building frequency

$R_2 = \dfrac{M_b}{M_t}$, ratio of equivalent building mass to total real mass

$R_3 = \dfrac{k_{xx}}{k_p}$, ratio of soil to pile stiffness

$R_4 = \dfrac{M_p}{M_t}$, ratio of pile mass to total real mass

$R_5 = \dfrac{c_{xx}}{k_{xx}}$, ratio of soil damping to soil stiffness (secs).

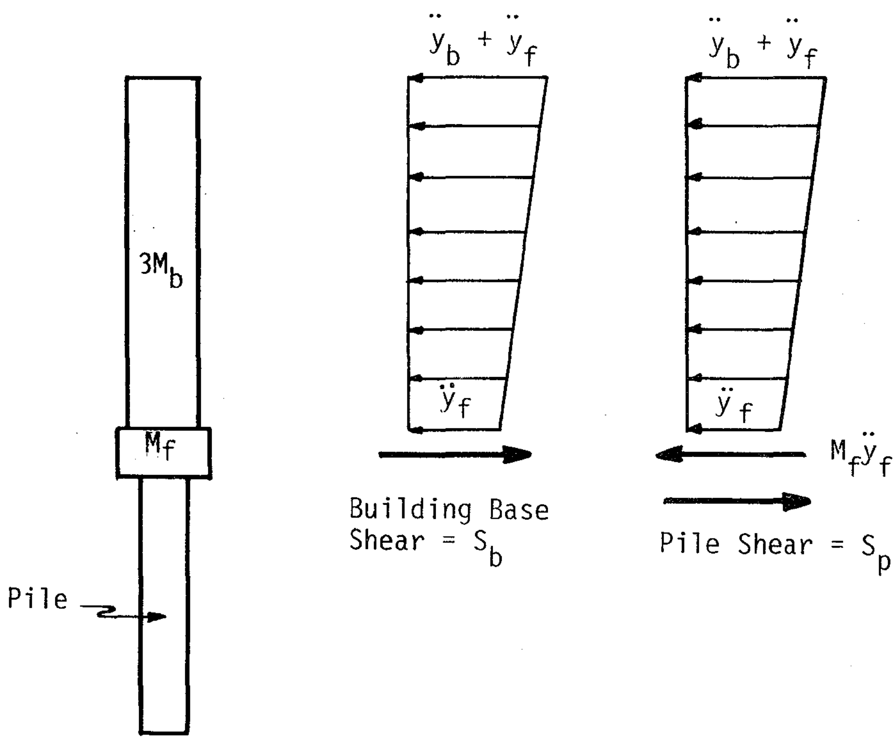

Fig. 4.2 Building Base Shear and Pile Shear

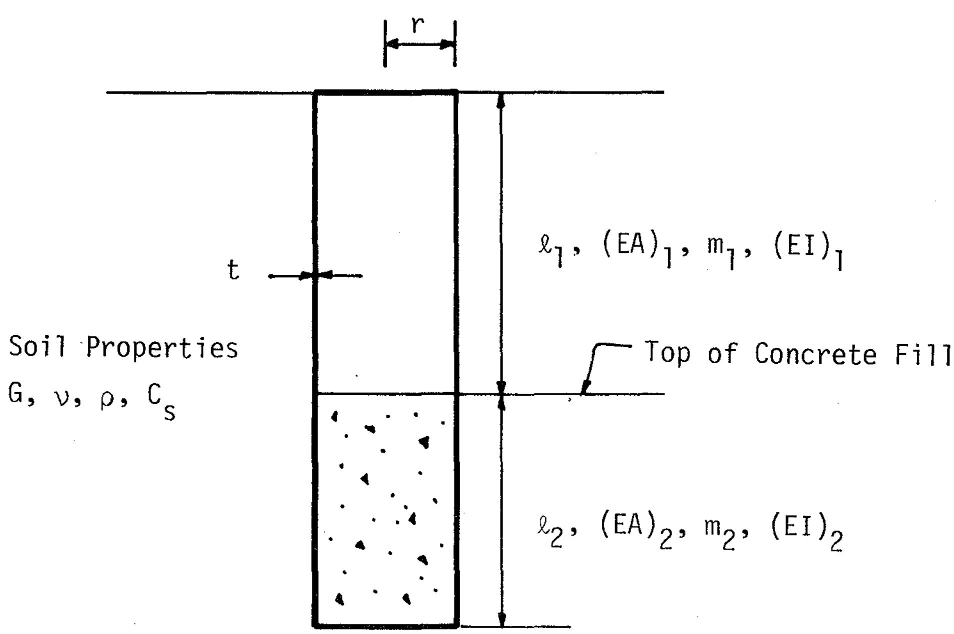

Fig. 4.3 Sleeve and Surrounding Soil Properties

The equivalent translational soil stiffness and corresponding equivalent viscous damping expressions for the vertical direction are the real and imaginary parts respectively of the following equation

$$k_{zz} = (EA)_1 \eta_1 \tanh \eta_1 \ell_1 + (EA)_2 \eta_2 \frac{1 + \frac{k_{zb}}{(EA)_2 \eta_2} \coth \eta_2 \ell_2}{\frac{k_{zb}}{(EA)_2 \eta_2} + \coth \eta_2 \ell_2} , \qquad (4.12)$$

where η_1, η_2, k_{zb} and k_{zs} are defined as

$$\eta_1 = \sqrt{\frac{k_{zs} - m_1 \Omega^2}{(EA)_1}} \qquad \text{(a)}$$

$$\eta_2 = \sqrt{\frac{k_{zs} - m_2 \Omega^2}{(EA)_2}} \qquad \text{(b)} \qquad (4.13)$$

$$k_{zs} = 2.3G + i(0.7 + \frac{6\Omega r}{C_s})G \qquad \text{(a)}$$

$$k_{zb} = \frac{4r}{1-\nu} G + i \left\{\frac{3.2 \, \Omega \, r^2}{(1-\nu)C_s}\right\} G \qquad \text{(b)} \qquad (4.14)$$

and Ω = the fundamental frequency of the vertical excitation

ν = Poisson's ratio of the soil medium

C_s = shear wave velocity of the soil medium

G = shear modulus of the soil medium

r = radius of the sleeve of thickness t_s

ℓ_1, ℓ_2 = length of the upper and lower portions of the sleeve

m_1, m_2 = mass per unit length of the upper and lower portions

$(EA)_1$ = Young's modulus of steel times the area of the sleeve (upper portion)

$(EA)_2$ = $(EA)_1$ + the equivalent effect of the concrete fill (lower portion)

The above expressions are for a single friction pile in an infinite half-space.

The length of the upper portion of the sleeve (ℓ_1) is taken to be the designed free length of the pile. Even with the soft soil assumed, the effect of soil flexibility on the vertical response is small.

4.3.2 Dynamic Stiffnesses of Pile

In determining the horizontal stiffness of the pile one has to include the effect of the axial force, the soil rotational stiffness and the coupling between the soil translational and rotational stiffnesses at the bottom of the free pile length (see Fig. 4.4). Referring to the Kaynia report (6), let k_{xx} and $k_{\phi\phi}$ define the translational and rotational dynamic stiffnesses and $k_{x\phi}$ as the coupling term. To account for the coupling effect, a rigid link of length $\delta = -k_{x\phi}/k_{xx}$ is added to the pile, and this is mounted on uncoupled translational and rotational springs k_{xx} and $k_{\phi\phi} - \delta^2 k_{xx}$ respectively (see Ref. (6)).

If ℓ and EI are the free length and bending rigidity of the pile, the equivalent stiffness of this member in the horizontal direction is given by

$$k_p = \frac{3EI}{\ell^3}\frac{a^3}{3}\frac{1 - ab\,(a\,\frac{\delta}{\ell} + \tan a)}{\left\{1 + (1 + \frac{\delta}{\ell})a^2 b\right\}\,(a\,\frac{\delta}{\ell} + \tan a) - a(1 + \frac{\delta}{\ell})}\,, \qquad (4.15)$$

where the dimensionless parameters a and b are defined as

$$a = \sqrt{\frac{P\ell^2}{EI}} \qquad (a)$$

$$b = \frac{EI}{\ell(k_{\phi\phi} - \delta^2 k_{xx})} \qquad (b) \qquad (4.16)$$

and P is the axial force in the pile. The axial load is a function of the vertical vibration and hence varies with time. This expression applies to pile type (1); constant diameter pile hinged at the top.

In this simplified analysis, the coupling of the translational and rotational stiffnesses is ignored. The expression for the equivalent horizontal stiffness of the pile simplifies to

$$k_p = \frac{3EI}{\ell^3}\frac{a^3}{3}\frac{1 - ab\tan a}{(1 + a^2 b)\tan a - a} , \tag{4.17}$$

where b is now defined as

$$b = \frac{EI}{\ell k_{\phi\phi}} . \tag{4.18}$$

In the present investigation the pile stiffness in the vertical direction is simply

$$k_{pz} = \frac{AE}{\ell} . \tag{4.19}$$

4.4 Numerical Analysis

4.4.1 Techniques

The integration scheme of the Newmark-Wilson θ method is implemented in a computer program to perform the time-history analysis. The Newmark and Wilson methods are implicit integration methods, the displacement solution at time $t + \Delta t$ is based on using the equilibrium conditions at time $t + \Delta t$,

$$M\ddot{U}_{t+\Delta t} + C\dot{U}_{t+\Delta t} + KU_{t+\Delta t} = F_{t+\Delta t} . \tag{4.20}$$

The complete algorithm using the Newmark-Wilson integration scheme is given in Table 4.1.

The parameters α, δ and θ are assigned the values of 1/6, 1/2, and 1.4 respectively. With $\theta \geq 1.37$ the integration scheme is unconditionally stable. The accuracy of the integration depends on the time step, Δt. A value of 0.01 seconds (which satisfies $\Delta t \leq T_p/2\pi$ where T_p is the highest period of the system) is used in all the time-history analyses.

The complete time-history analysis for the vertical ground motion is performed first. Then the time-history analysis for the horizontal ground motion is performed using the dynamic pile axial load from the vertical analysis at each time step to calculate the equivalent pile stiffness in the horizontal direction.

4.4.2 Scaling of Results

It is not the intent here to investigate the effects of earthquakes of differing strengths. Therefore, the time-history results are scaled so as to be consistent with the design assumption. However, these results serve to evaluate the design procedure based on a simple one-degree model and to investigate the effect of differing frequency content, duration, etc. of real ground motions.

It will be recalled that the design value of maximum pile displacement was computed as the peak ground displacement (assumed to be 30.48 cm) times the displacement amplification ratio (obtained from the smoothed design spectra). Now approximate the pile displacement for a particular earthquake as the response displacement obtained from the response spectrum of that earthquake at the period of the one-degree model. The scaling factor is thus taken to be the ratio of the two pile displacements,

$$\xi = \frac{\text{design pile displacement}}{\text{earthquake pile displacement}} \quad .$$

The scaling factors for the four horizontal earthquake records used in these time-history analyses are presented in Table 4.2.

	Earthquake Record	Period of the One-Degree Design Model (seconds)		
		8	10	12
Pile Damping Ratio 0.5%	EQ-1 (H)	.6897	1.0109	.9391
	EQ-2 (H)	.8398	1.0999	1.1391
	EQ-3 (H)	1.3601	.6930	.5748
	EQ-4 (H)	2.1719	1.6750	2.0971
Pile Damping Ratio 0.10%	EQ-1 (H)	.7158	.7045	.6978
	EQ-2 (H)	.9077	.8297	.8707
	EQ-3 (H)	1.3316	.9104	.8495
	EQ-4 (H)	2.4612	1.8542	2.0840

Table 4.2 Scaling Factors

Earthquake Record	Design Period (seconds)			Design Period (seconds)		
	8	10	12	8	10	12
EQ-1	50.0 (0.051g)	51.7 (0.053g)	41.8 (0.043g)	46.7 (0.048g)	33.3 (0.034g)	22.9 (0.023g)
EQ-2	49.8 (0.051g)	34.7 (0.035g)	26.4 (0.027g)	48.4 (0.049g)	30.0 (0.031g)	19.2 (0.020g)
EQ-3	54.0 (0.055g)	27.9 (0.028g)	16.5 (0.017g)	50.5 (0.051g)	27.0 (0.028g)	15.9 (0.016g)
EQ-4	48.3 (0.049g)	29.2 (0.030g)	20.4 (0.021g)	46.9 (0.048g)	27.4 (0.028g)	17.2 (0.018g)
	Acceleration at Building Top (cm/sec^2)			Building Base Shear/Building Mass (cm/sec^2)		

EQ-1	1.77	1.27	.73	46.6 (0.047g)	37.8 (0.039g)	27.0 (0.028g)
EQ-2	1.84	1.10	.85	48.2 (0.049g)	32.2 (0.033g)	21.0 (0.021g)
EQ-3	1.91	1.02	.60	51.1 (0.052g)	27.1 (0.028g)	16.0 (0.016g)
EQ-4	1.75	1.03	.62	47.1 (0.048g)	27.9 (0.028g)	18.2 (0.019g)
	Building Displacement (cm)			Pile Shear/Total Mass (cm/sec^2)		

EQ-1	75.1	71.3	61.2	372	442	450
EQ-2	77.3	69.7	59.8	387	419	432
EQ-3	78.8	67.1	57.0	411	385	381
EQ-4	74.0	67.6	56.8	409	422	444
	Pile Displacement (cm)			Pile Stress (MPa)		

Table 4.3 Time-History Analysis Results; Case A, $\beta_p = 0.5\%$, $f_Y = 414$ MPa, $P = 1.11$ MN
Vertical and Horizontal Vibrations

		CASE A			CASE B		
Design Period		8	10	12	8	10	12
Horizontal Modes	T_1	8.04	10.03	12.03	8.04	10.03	12.03
	T_2	0.659	0.660	0.660	0.659	0.660	0.660
	T_3	0.00783	0.00784	0.00784	0.0111	0.0111	0.0111
Vertical Modes	T_1	0.219	0.220	0.220	0.233	0.235	0.235
	T_2	0.0679	0.0688	0.0695	0.0829	0.0838	0.0845
	T_3	0.00487	0.00499	0.00512	0.00683	0.00701	0.00717

Table 4.5

The pile design and pile response values of displacement, acceleration (pile shear per total mass) and stress are summarized below for convenience of the comparison. The pile design values are from Table 3.2; the pile response values from Tables 4.3 and 4.4. Two response values are tabulated for each pile period; the high and the average of the four earthquake pair responses.

	pile period (secs)	pile design value	pile response (average)	pile response high
pile displacement (cm)	8	82.3	76.3	78.8
	10	71.6	69.9	77.1
	12	61.0	58.7	61.3
pile acceleration (cm/sec^2)	8	50.9	48.2	51.1
	10	28.4	31.2	38.9
	12	16.8	20.4	27.8
pile stress (MPa) (for all periods)	Table 4.3	414	413	450
	Table 4.4	689	684	738

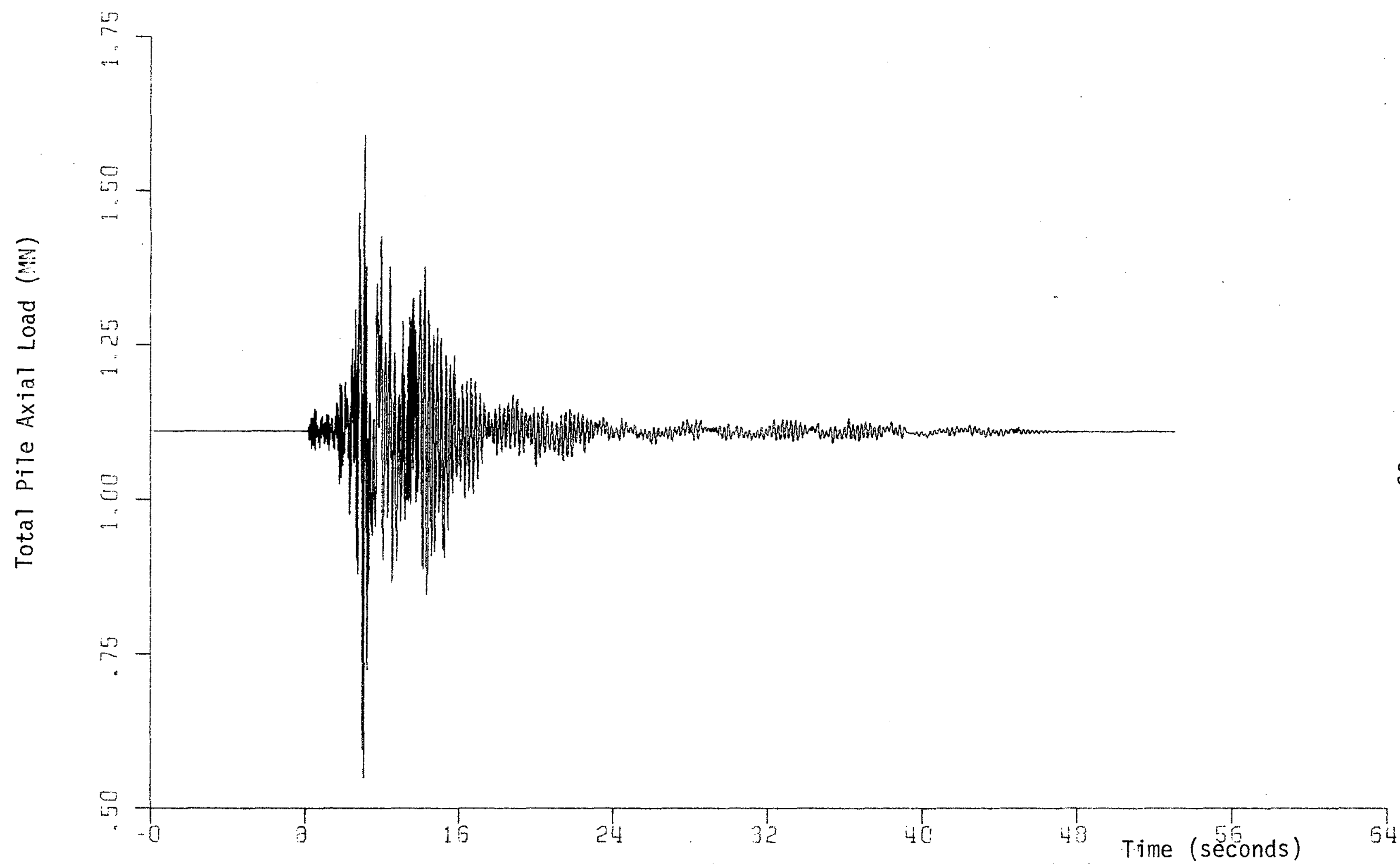

Fig. 4.5 Time-History Response — Total Pile Axial Load (MN)
Pile Design Case A; f_y = 414 MPa, P = 1.11 MN, t = 2.54 cm;
T_p = 10 secs.; β_p = 0.5%. EQ-1.

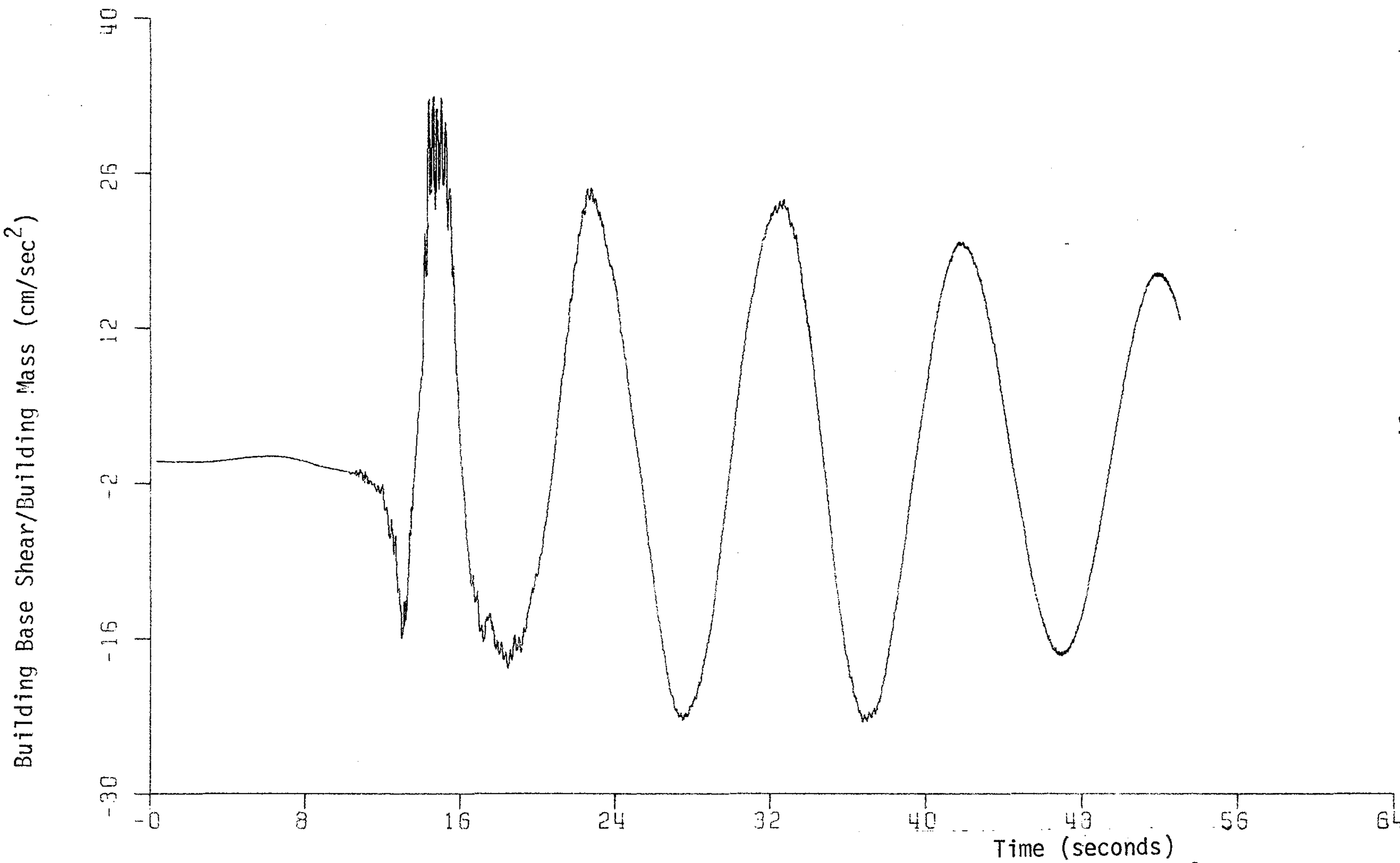

Fig. 4.7 Time-History Response — Building Base Shear/Building Mass (cm/sec^2)
Pile Design Case A; f_y = 414 MPa, P = 1.11 MN, t = 2.54 cm; T_p = 10 secs.;
β_p = 0.5%. EQ-1.

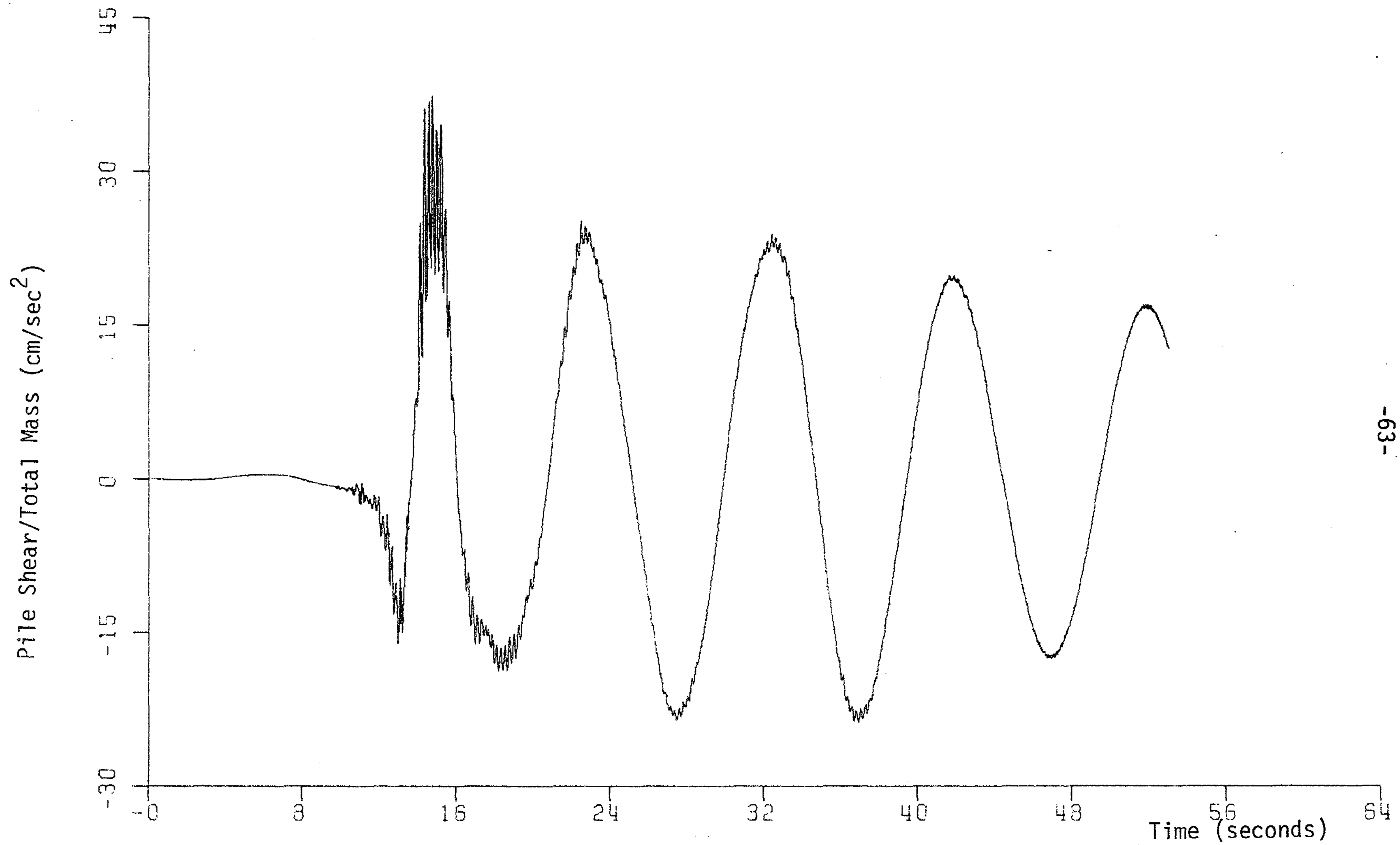

Fig. 4.9 Time-History Response — Pile Shear/Total Mass (cm/sec^2)
Pile Design Case A; f_y = 414 MPa, P = 1.11 MN, t = 2.54 cm;
T_p = 10 secs.; β_p = 0.5%. EQ-1.

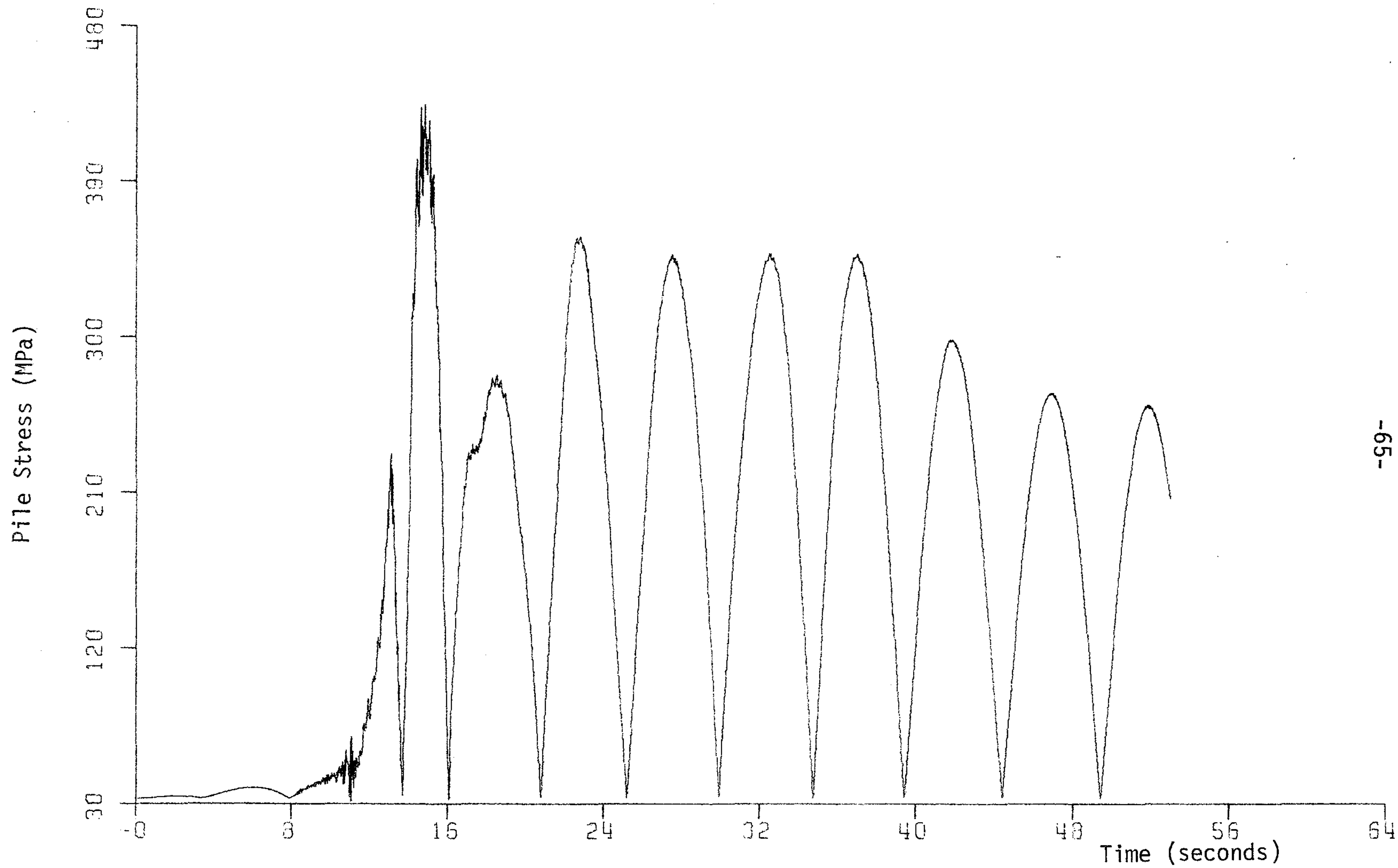

Fig. 4.11 Time-History Response — Pile Stress (MPa)
Pile Design Case A; f_y = 4.14 MPa, P = 1.11 MN,
t= 2.54 cm; T_p = 10 secs.; β_p = 0.5%. EQ-1.

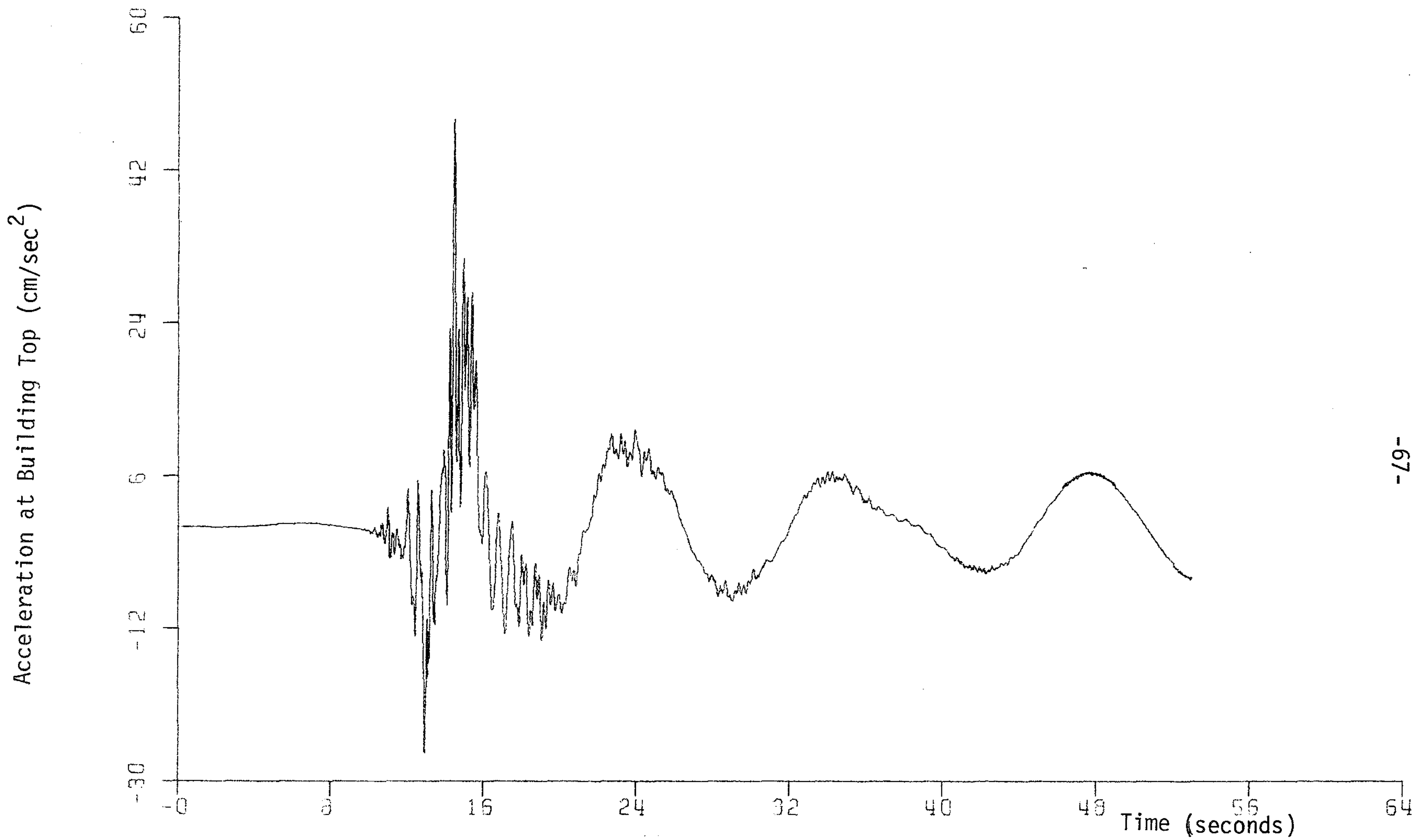

Fig. 4.13 Time-History Response — Acceleration at Building Top (cm/sec^2) Pile Design Case G; f_y = 689 MPa, P = 2.22 MN, t = 2.54 cm; T_p = 12 secs.; β_p = 0.5%. EQ-1.

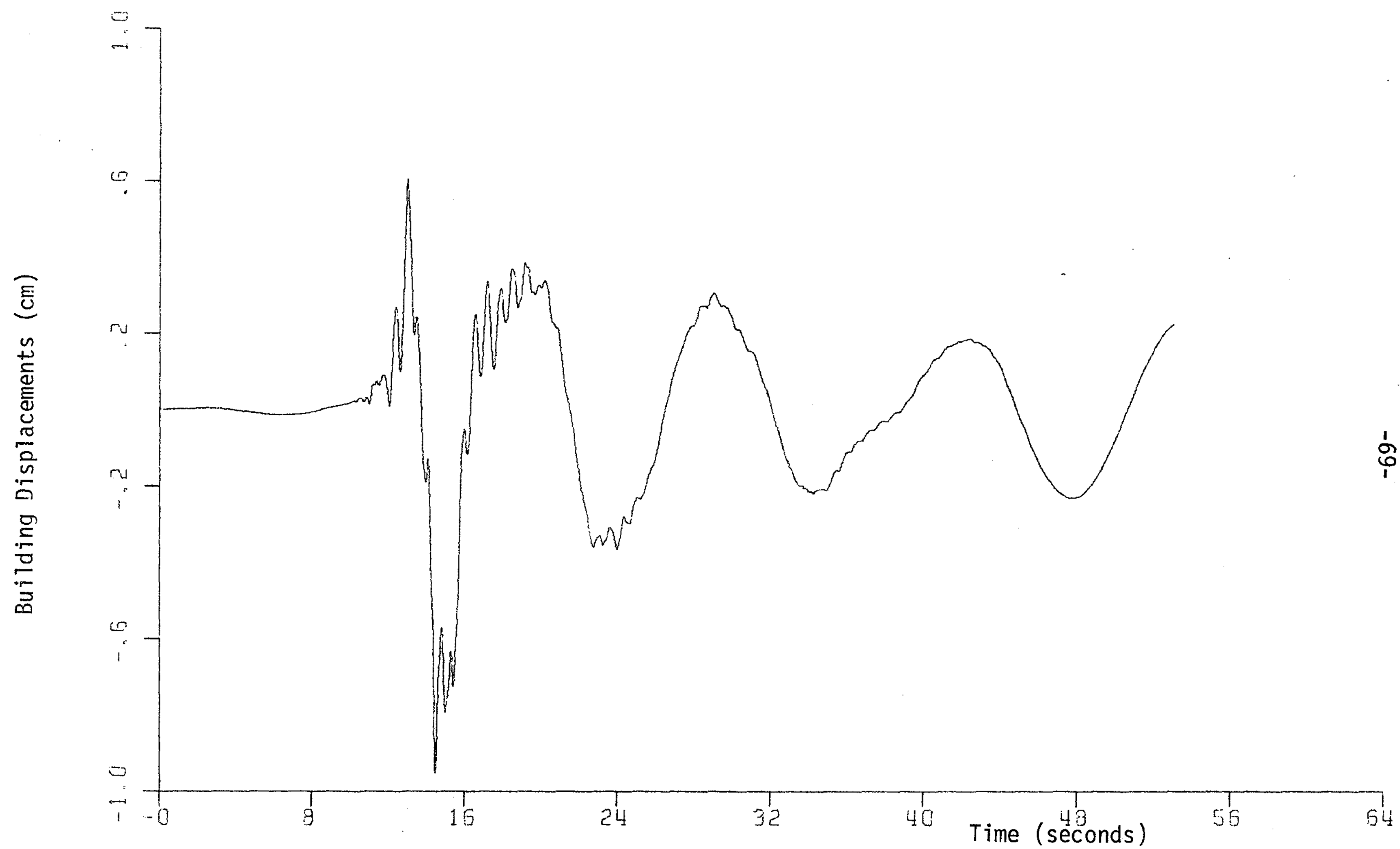

Fig. 4.15 Time-History Response — Building Displacement (cm)
Pile Design Case G; f_y = 689 MPa, P = 2.22 MN, t = 2.54 cm;
T_p = 12 secs.; β_p = 0.5%. EQ-1.

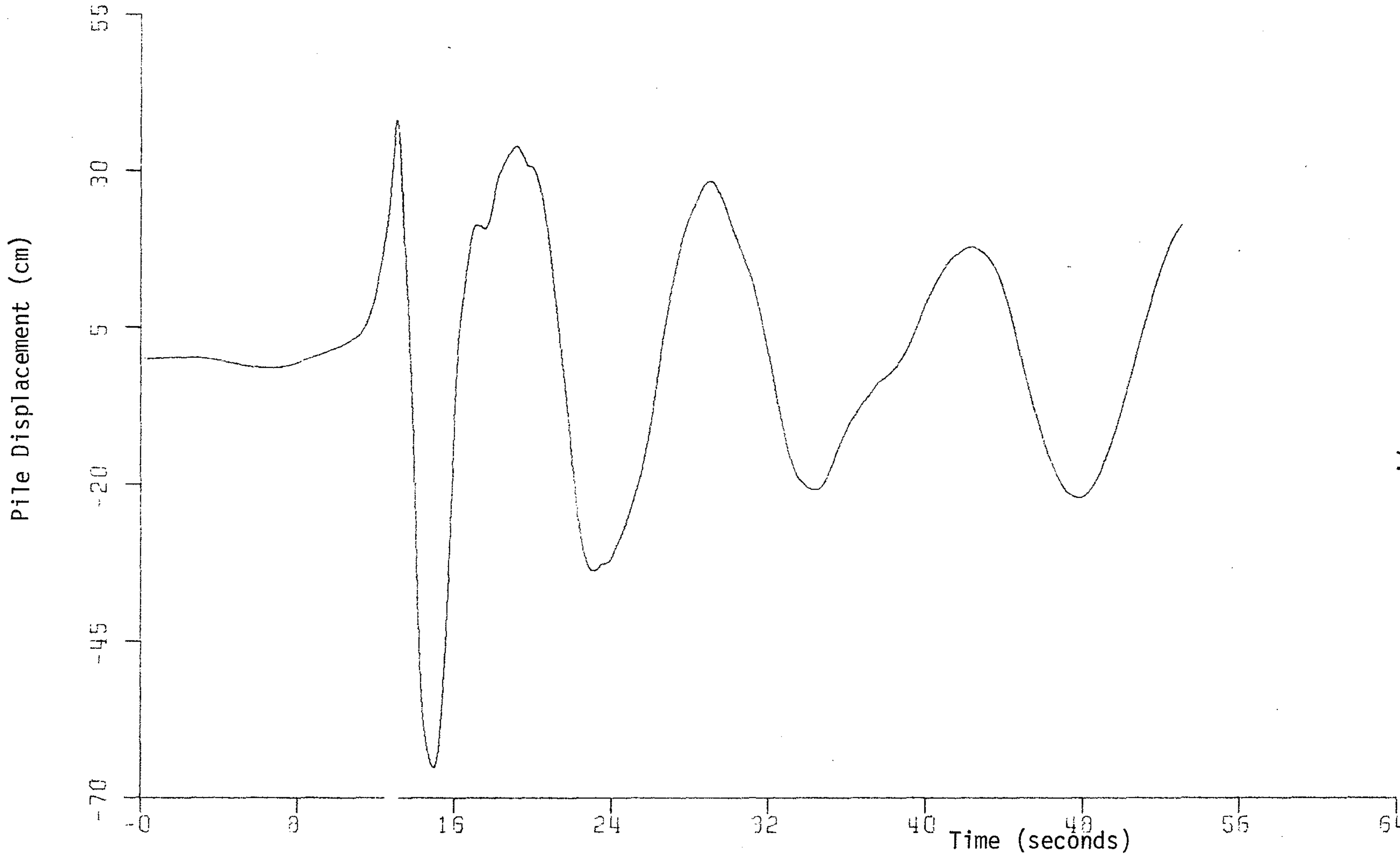

Fig. 4.17 Time-History Response — Pile Displacement (cm)
Pile Design Case G; f_y = 689 MPa, P = 2.22 MN, t = 2.54 cm;
T_p = 12 secs.; β_p = 0.5%. EQ-1.

Again, the second mode and the vertical motion are responsible for the high frequency response noted in the early phase of the building base shear/building mass and pile shear/total mass time histories, Figs. 4.7 and 4.9. However, the fundamental mode dominates the responses.

The time history of the pile displacement response, Fig. 4.10, shows very little, if any, higher frequency component. The response is governed primarily by the fundamental mode.

The pile stress time history, Fig. 4.11, reflects the absolute maximum stress in the pile which is always compression and may occur on either extreme point of the cross-section depending upon the direction of motion. The minimum value in the plot is simply the static P/A stress. The pile stress shows the high frequency response due to the second mode and the vertical vibrations in the first cycle after which the fundamental mode governs. However, this has little effect on the maximum pile stress.

All the building and pile responses peak between 14.4 and 14.9 seconds.

Figs. 4.12 through 4.18 show the building and pile response time histories for a 12 second period pile design. Note the increased effect of the higher modes. The vertical motion causes a greater effect on the responses for a 12 second design period than for 10 seconds. The peak responses for the two periods occur at essentially the same time.

Overall, the pile stress is less affected by the high modes and the vertical motion than the building acceleration, displacement and base shear, and the pile displacement and shear. This suggests a counterbalancing effect of the axial force (P-Δ effect) and the inertia or shear force in the pile stress computation. If the dynamic axial force in the pile increases, for example, the reduced pile stiffness decreases the moment due to the horizontal inertia force, thus partly counteracting the increased P-Δ moment.

4.6 Comparison with Code Design Practice

Current practice in earthquake design is embodied in design codes. As an example of a commonly used code, we shall consider the Uniform Building Code (1979). Essentially, the procedure is based on only the first mode of the structure. By assuming a characteristic shape for the first mode, it is possible to convert the maximum condition of response into a set of equivalent static forces. The actual design may then be executed on the basis of static analysis.

With T = 1 second, the maximum acceleration at the building top implied by the Code is equal to 0.13g (131 cm/sec^2), and the maximum building displacement is 3.3 cm. The maximum building base shear per building mass is equivalent to the average acceleration of the building, 0.067g (65 cm/sec^2). These values are all considerably larger than for the buildings designed with flexible pile foundations (see Tables 4.3 and 4.4).

In the present study the design values of pile displacement and acceleration are based on an assumed peak ground displacement of 30.48 cm. This value of the peak ground displacement is chosen arbitrarily and is not intended to be a recommended design value. However, 30.48 cm appears reasonable for many sites and for the purpose of the present study. The building response values therefore in general can not be directly compared with the standard code design values.

A conventional building designed according to current codes will receive considerable plastic deformation in a severe earthquake. However, a building on a horizontally flexible foundation, such as a sleeved-pile system, can be designed for even smaller lateral forces and yet the earthquake response is essentially elastic.

4.7 Effect of Vertical Ground Motion

The horizontal pile stiffness is a function of the pile axial load. The vertical ground motion causes variations in the pile axial load and thus has a direct effect on the horizontal pile stiffness and in turn on the response of the system to horizontal vibration. At any given time, the pile axial load is the sum of the static load, which corresponds to the total real mass, and a dynamic load due to the vertical vibration. To evaluate this effect, analyses were made for horizontal motion only.

The building and pile peak responses for horizontal ground motion only are tabulated in Tables 4.6 and 4.7, for pile design cases A and G, with β_p = 0.5%. Comparison of these values with those tabulated in Tables 4.3 and 4.4 reveals that the effect of the vertical motion is not very significant. In general, inclusion of the vertical motion increases the acceleration at the building top, causes a modest increase in base shear, but has little effect on pile stress or displacement.

Earthquake Record	Design Period (seconds) 8	10	12	Design Period (seconds) 8	10	12
EQ-1	46.8 (0.048g)	36.7 (0.037g)	22.6 (0.023g)	46.4 (0.047g)	29.7 (0.030g)	18.0 (0.018g)
EQ-2	48.9 (0.050g)	30.1 (0.031g)	18.4 (0.019g)	48.1 (0.049g)	28.4 (0.029g)	17.2 (0.018g)
EQ-3	49.6 (0.051g)	26.9 (0.027g)	15.8 (0.016g)	49.1 (0.050g)	26.7 (0.027g)	15.7 (0.016g)
EQ-4	47.4 (0.048g)	27.8 (0.028g)	16.8 (0.017g)	46.6 (0.047g)	27.3 (0.028g)	16.5 (0.017g)

Acceleration at Building Top (cm/sec^2) — Building Base Shear/Building Mass (cm/sec^2)

EQ-1	1.76	1.21	.73	46.3 (0.047g)	27.2 (0.028g)	16.9 (0.017g)
EQ-2	1.83	1.09	.65	47.9 (0.049g)	28.0 (0.029g)	16.9 (0.017g)
EQ-3	1.85	1.01	.59	49.0 (0.050g)	26.7 (0.027g)	15.7 (0.016g)
EQ-4	1.75	1.02	.60	46.4 (0.047g)	27.4 (0.028g)	16.4 (0.017g)

Building Displacement (cm) — Pile Shear/Total Mass (cm/sec^2)

EQ-1	74.6	70.6	60.4	620	687	686
EQ-2	77.2	70.1	60.2	648	688	699
EQ-3	78.6	66.9	56.5	687	634	619
EQ-4	73.8	67.7	56.8	695	705	737

Pile Displacement (cm) — Pile Stress (MPa)

Table 4.7 Time-History Analysis Results; Case G, $\beta_p = 0.5\%$
Horizontal Vibration Only

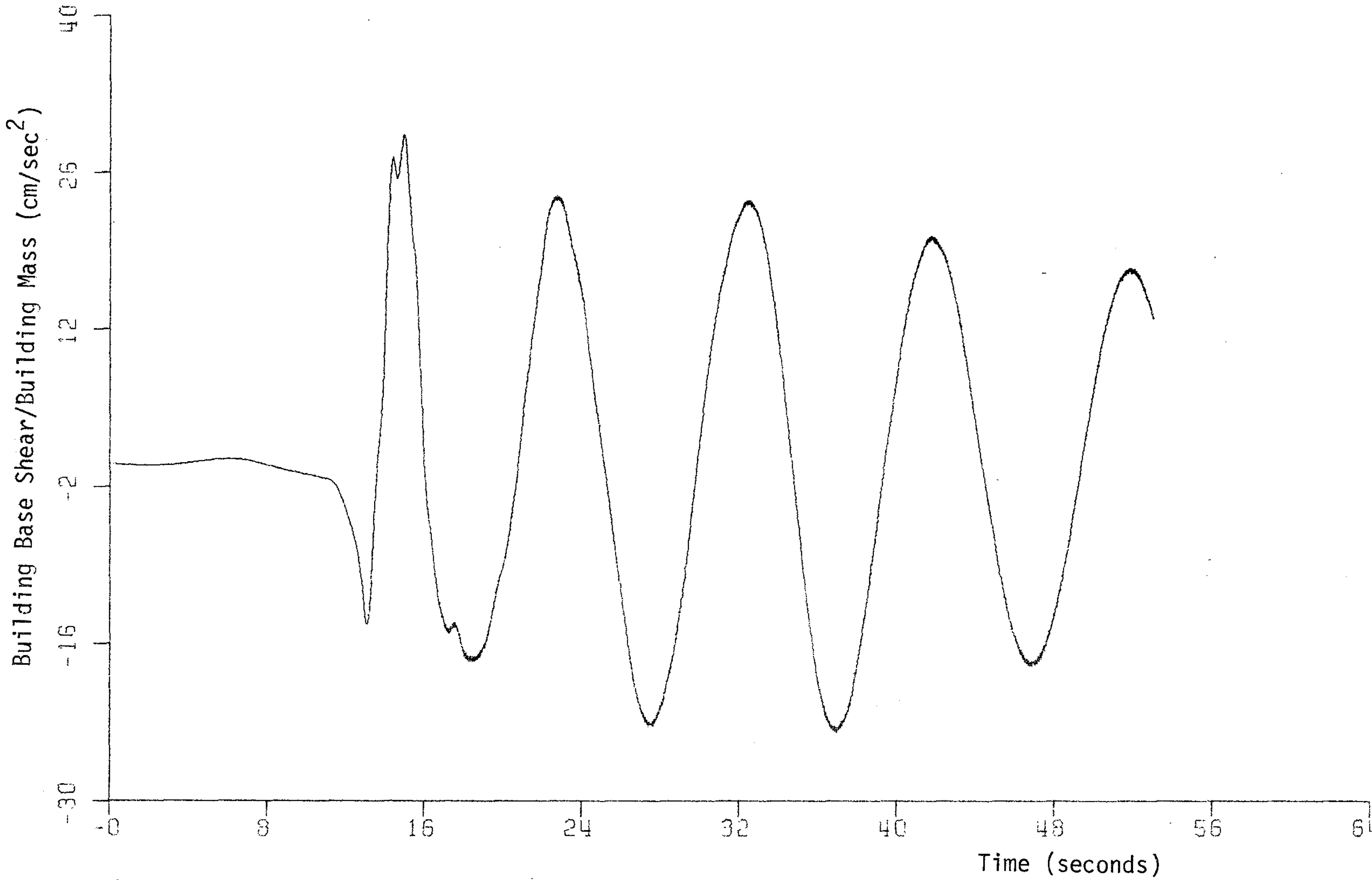

Fig. 4.21 Time-History Response — Building Base Shear/Building Mass (cm/sec^2) Pile Design Case A; f_y = 414 MPa, P = 1.11 MN, t = 2.54 cm; T_p = 10 secs.; β_p = 0.5%. EQ-1.

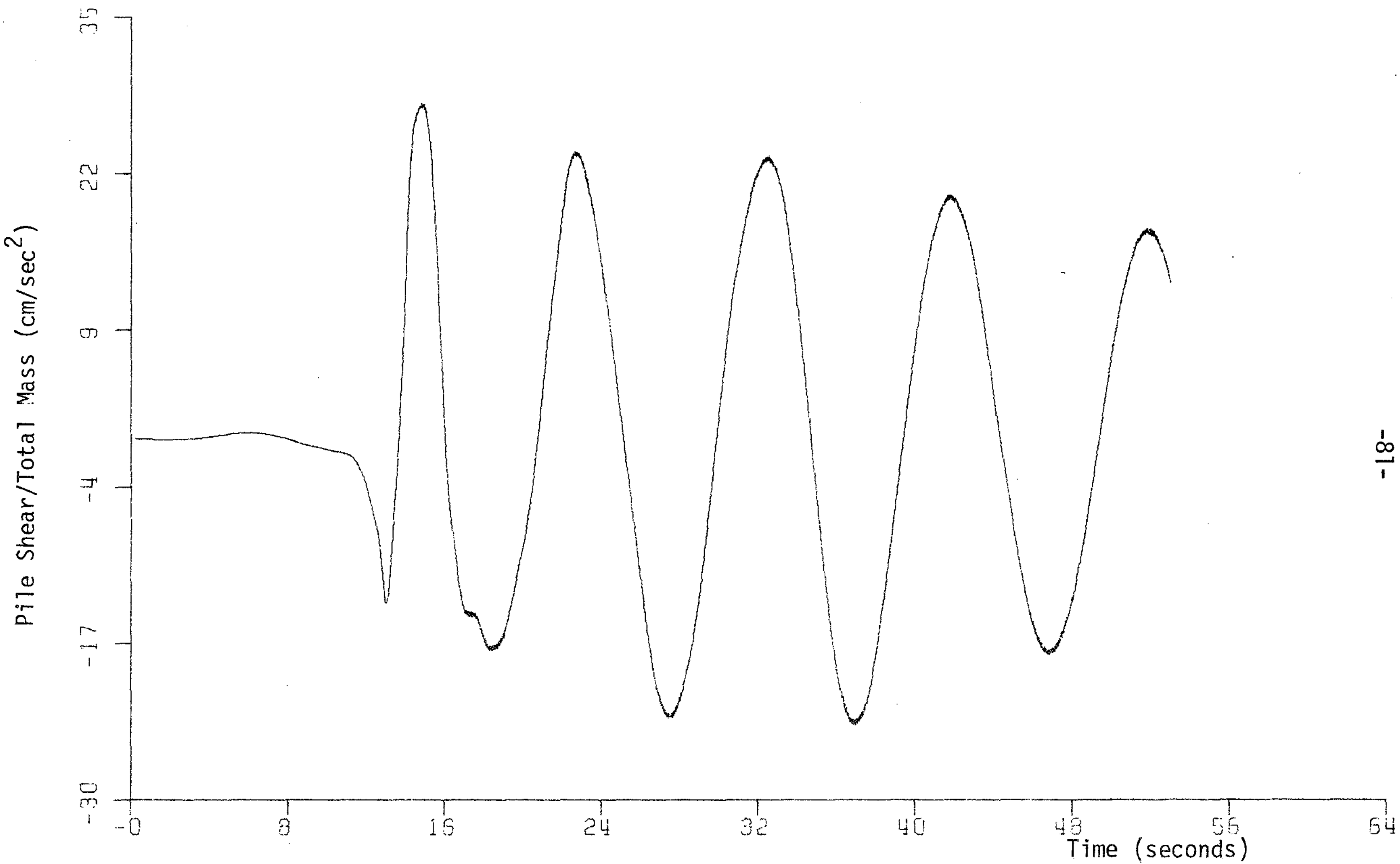

Fig. 4.23 Time-History Response — Pile Shear/Total Mass (cm/sec^2)
Design Pile Case A; f_y = 414 MPa, P = 1.11 MN, t = 2.54 cm;
T_p = 10 secs.; β_p = 0.5%. EQ-1.

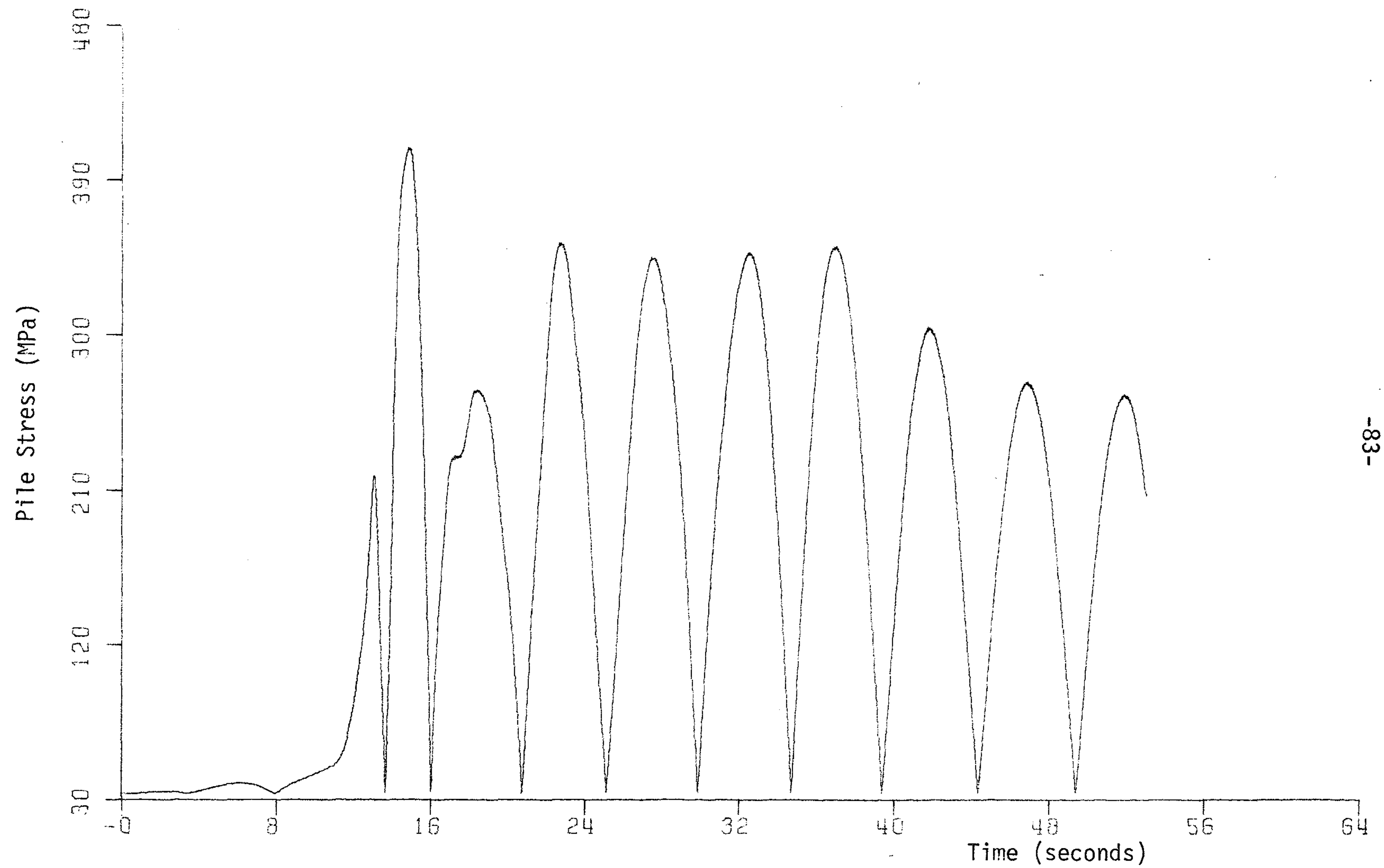

Fig. 4.25 Time-History Response — Pile Stress (MPa)
Pile Design Case A; f_y = 414 MPa, P = 1.11 MN,
t = 2.54 cm; T_p = 10 secs.; β_p = 0.5%. EQ-1.

Acceleration at Building Top (cm/sec^2)

Earthquake Record	Horizontal Building Period (seconds) 1	2	3
EQ-1	51.7 (0.053g)	47.5 (0.048g)	70.9 (0.072g)
EQ-2	34.7 (0.035g)	52.1 (0.053g)	48.4 (0.049g)
EQ-3	27.9 (0.028g)	28.4 (0.029g)	28.1 (0.029g)
EQ-4	29.2 (0.030g)	29.3 (0.030g)	29.1 (0.030g)

Building Base Shear/Building Mass (cm/sec^2)

Earthquake Record	Horizontal Building Period (seconds) 1	2	3
EQ-1	33.3 (0.034g)	37.3 (0.038g)	38.5 (0.039g)
EQ-2	30.0 (0.031g)	32.6 (0.033g)	31.6 (0.032g)
EQ-3	27.0 (0.028g)	27.2 (0.028g)	26.8 (0.027g)
EQ-4	27.4 (0.028g)	27.0 (0.028g)	26.7 (0.027g)

Building Displacement (cm)

Earthquake Record	1	2	3
EQ-1	1.27	4.83	15.5
EQ-2	1.10	5.69	11.8
EQ-3	1.02	4.12	9.11
EQ-4	1.03	4.02	8.93

Pile Shear/Total Mass (cm/sec^2)

Earthquake Record	1	2	3
EQ-1	37.8 (0.039g)	41.9 (0.043g)	33.5 (0.034g)
EQ-2	32.2 (0.033g)	30.4 (0.031g)	29.4 (0.030g)
EQ-3	27.1 (0.028g)	27.2 (0.028g)	26.8 (0.027g)
EQ-4	27.9 (0.028g)	27.6 (0.028g)	25.9 (0.026g)

Pile Displacement (cm)

Earthquake Record	1	2	3
EQ-1	71.3	69.7	65.1
EQ-2	69.7	67.8	64.7
EQ-3	67.1	67.3	67.2
EQ-4	67.6	65.8	63.0

Pile Stress (MPa)

Earthquake Record	1	2	3
EQ-1	442	430	399
EQ-2	419	407	393
EQ-3	385	386	385
EQ-4	422	412	397

Table 4.8 Effect of Building Period; Case A, $T_p = 10^s$, $\beta_p = 0.5\%$
Vertical and Horizontal Vibrations

4.9 Effect of Wind-Resisting Devices

It is necessary to devise a method to accommodate wind loads without excessive building motion by a stiffer system to be active only under these forces. The extent of the present study is to determine the effect of a rigid-brittle wind-resisting device on the performance of the modeled system under earthquake ground motions. This high-stiffness, limited strength wind shear element would render itself inactive in the event of an earthquake producing large base forces. The limit of its strength will be determined as a function of the building size and type. The purpose is not to study wind effects on buildings, but it is necessary to consider the effect of this initial condition on the response to earthquake ground motions.

With the wind-resisting device functional, the building superstructure and foundation system can be modeled as a one-degree system (see Fig. 4.26).

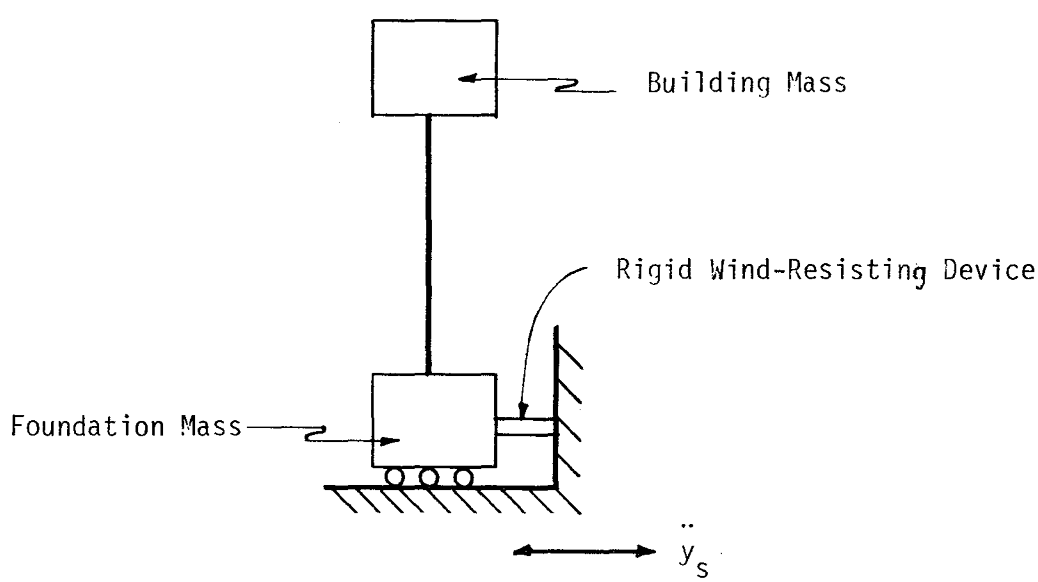

Fig. 4.26 Wind-Resisting Device

The strength of the wind-resisting device is a function of the building size. Let $p(N/m^2)$ define the design wind pressure. The real building mass per square foot of frontal area is expressed by $w\rho/g$, where w and ρ are the building width (parallel to the wind) and its density. The expression for the design wind force per building mass is then given by

$$\left(\frac{R}{3M_b}\right)_d = \frac{pg}{w\rho} \quad . \tag{4.26}$$

Let the values of the parametsrs (p, w, ρ) be such as to maximize the expression for $(R/3M_b)_d$, say $p = 1200\ N/m^2$, $w = 28\,m$, $\rho = 1400\ N/m^3$. On this basis, a reasonable maximum value is probably $(R/3M_b)_d = 30.5\ cm/sec^2$. This value is used to estimate the maximum possible effect. If this effect on the performance of the system is not significant, there is no need for further investigation.

The procedure begins with time-history analysis of the one-degree system (Fig. 4.26). When the computed wind-resisting force per building mass (Eq. 4 .25)) exceeds the limiting value, the device ceases to function and the system responds as a three-degree system. The analysis proceeds as before (Section 4.2) with the initial conditions existing in the one-degree analysis at the time of the break.

The building and pile response values for the model with and without the wind-resisting device are tabulated in Tables 4.10 and 4.11. Table 4.10 corresponds to pile design case A, with $T_p = 10$ seconds and $\beta_p = 0.5\%$, and Table 4.11 to pile design case G, with $T_p = 12$ seconds and $\beta_p = 0.5\%$.

The inclusion of the rigid-brittle wind-resisting device in the analysis has no significant effect on the peak responses of the model except on the building acceleration due to EQ-4. This appears to be a unique occurrence. The building base shear is not significantly affected.

Figs. 4.28 and 4.29 are the time histories of the acceleration at the building top and the pile stress for pile design case A, with $T_p = 10$ seconds and $\beta_p = 0{,}5\%$. The earthquake pair EQ-1 is used in the time-history analysis.

Earthquake Record	With Wind-Resisting Device	Without Wind-Resisting Device	With Wind-Resisting Device	Without Wind-Resisting Device
EQ-1	41.9 (0.042g)	45.2 (0.046g)	23.7 (0.024g)	23.6 (0.024g)
EQ-2	39.3 (0.040g)	24.3 (0.025g)	22.9 (0.023g)	18.3 (0.018g)
EQ-3	20.6 (0.021g)	18.6 (0.019g)	14.8 (0.015g)	15.9 (0.016g)
EQ-4	71.8 (0.073g)	21.8 (0.022g)	35.0 (0.036g)	17.0 (0.017g)

Building Acceleration at Top (cm/sec²) — Building Base Shear/Building Mass (cm/sec²)

EQ-1	.85	.90	28.9 (0.029g)	27.8 (0.028g)
EQ-2	.77	.73	20.0 (0.020g)	18.5 (0.019g)
EQ-3	.56	.60	14.9 (0.015g)	16.1 (0.016g)
EQ-4	.99	.64	18.2 (0.019g)	18.7 (0.019g)

Building Displacement (cm) — Pile Shear/Total Mass (cm/sec²)

EQ-1	62.7	61.3	745	729
EQ-2	63.5	59.8	737	701
EQ-3	52.9	57.1	582	625
EQ-4	59.5	56.7	765	738

Pile Displacement (cm) — Pile Stress (MPa)

Table 4.11 Effect of Wind-Resisting Device; Case G, $T_p = 12^s$, $\beta_p = 0.5\%$ Vertical and Horizontal Vibrations

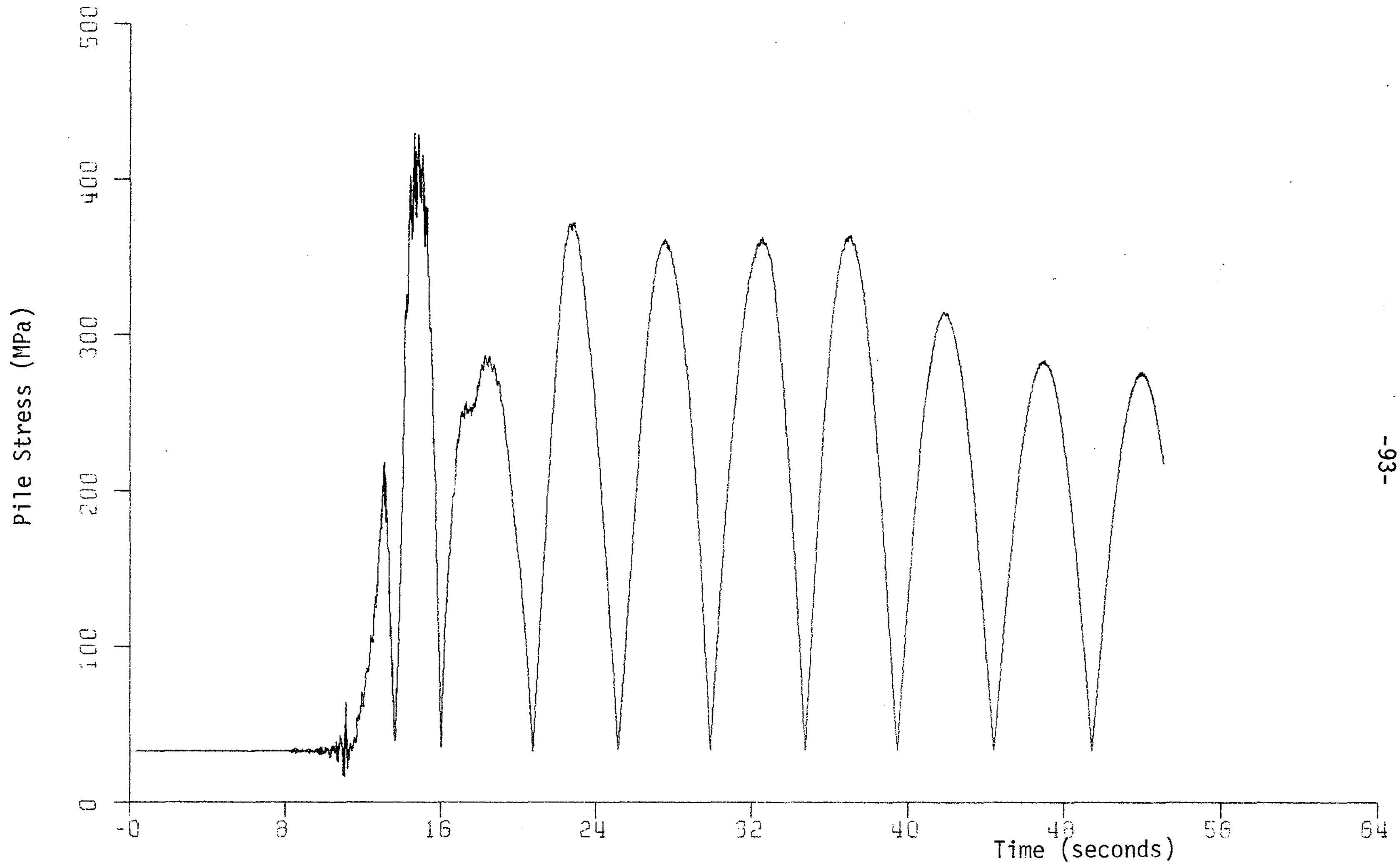

Fig. 4.29 Time-History Response —— Pile Stress (MPa)
Pile Design Case A; f_y = 414 MPa, P = 1.11 MN,
t = 2.54 cm; T_p = 10 secs., β_p = 0.5%. EQ-1.

Earthquake Record	Building Acceleration at Top (cm/sec²), Pile Damping Ratio 0.5%	Building Acceleration at Top (cm/sec²), Pile Damping Ratio 10%	Building Base Shear/Building Mass (cm/sec²), Pile Damping Ratio 0.5%	Building Base Shear/Building Mass (cm/sec²), Pile Damping Ratio 10%
EQ-1	51.7 (0.053g)	47.0 (0.048g)	33.3 (0.034g)	27.2 (0.028g)
EQ-2	34.7 (0.035g)	26.2 (0.027g)	30.0 (0.031g)	21.4 (0.022g)
EQ-3	27.8 (0.028g)	22.9 (0.023g)	27.0 (0.028g)	19.9 (0.020g)
EQ-4	29.2 (0.030g)	26.7 (0.027g)	27.4 (0.028g)	21.0 (0.021g)

Earthquake Record	Building Displacement (cm), 0.5%	Building Displacement (cm), 10%	Pile Shear/Total Mass (cm/sec²), 0.5%	Pile Shear/Total Mass (cm/sec²), 10%
EQ-1	1.27	1.10	37.8 (0.039g)	30.4 (0.031g)
EQ-2	1.10	.79	32.2 (0.033g)	22.3 (0.023g)
EQ-3	1.02	.76	27.1 (0.028g)	19.6 (0.020g)
EQ-4	1.03	.80	27.9 (0.028g)	21.4 (0.022g)

Earthquake Record	Pile Displacement (cm), 0.5%	Pile Displacement (cm), 10%	Pile Stress (MPa), 0.5%	Pile Stress (MPa), 10%
EQ-1	71.3	46.0	442	434
EQ-2	69.7	45.0	419	408
EQ-3	67.1	45.0	385	409
EQ-4	67.6	45.1	422	454

Table 4.12 Effect of Pile Damping Ratio; Case A, T_p = 10 seconds Vertical and Horizontal Vibrations

	design period (seconds)	design value	response value
pile displacement (cm):	10	45.7	45.3
	12	42.7	42.7
pile acceleration (cm/sec^2):	10	18.1	23.4
	12	11.7	17.9
pile stress (MPa):	Table 4.12	414	426
(for all periods)	Table 4.13	689	712

The pile displacement response is essentially identical to the design value. A greater pile acceleration results from the time-history analysis than design for, yet the resulting pile stress increase is insignificant. Therefore the pile design procedure is valid for higher pile damping ratios, at least up to 10%.

CHAPTER V - CONCLUSIONS

The studies reported herein demonstrate the effectiveness of flexible foundation design in reducing the seismic forces on the building superstructure. Sleeved piles, designed to produce a fundamental period in the 8-12 second range, reduce the forces below those normally used in conventional Code designs, even though the building remains essentially elastic during a severe earthquake. Time-history analyses, using real earthquake records processed so as to be reliable in the long period range, show that for a peak ground displacement of 30.5 cms (1 ft) the building base shear corresponds to accelerations of only about 0.02 to 0.05g.

Only the sleeved-pile concept has been investigated here. Other devices, such as rubber bearing pads, might produce the same benefits and could possibly be more economical. However, this concept has the advantage of reliability, since it depends only on the elastic behavior of steel.

A simple pile design procedure, based on a one-degree model and smoothed horizontal design spectra, has been developed and is presented in Chapter III. The time-history analyses verify the adequacy of the procedure, i.e., it accurately predicts the pile displacements and stresses. It also satisfactorily predicts the building base shear, although it cannot predict the distribution of forces over the building height.

Investigations of various effects on system behavior lead to the following conclusions: (1) Vertical ground motion, which is included in these studies, changes the system response in the early stages but has little effect on the peak pile stresses or building base shear. (2) The natural period of the building has little effect on the pile design within the range considered (1-3 seconds). (3) A rigid-brittle wind-resisting device, having a strength equal to the maximum design wind force, has little effect on earthquake response. (4) The simple design procedure is also adequate for high pile damping which might be provided by special devices.

For efficient and effective design, it is advantageous to achieve a long period and to use high-strength steel in the pile. Periods even longer than the maximum used here (12 seconds) might be desirable. That limit is imposed only because the earthquake records, even after processing, are not

References

1. Fintel, M., and Khan, R.R., "Shock-Absorbing Soft-Story Concept for Multistory Earthquake Structures," Journal of the American Concrete Institute, Vol. 66-5, May 1969.

2. Chopra, A.K., Clough, D.P., and Clough, R.W., "Earthquake Resistance of Buildings with a "Soft" First Story," Earthquake Engineering and Structural Dynamics, Vol. 1-4, April-June 1973.

3. Crandall, S.H., Lee, S.S., and Williams, J.H., "Accumulated Slip of a Friction-Controlled Mass Excited by Earthquake Motions," Journal of Applied Mechanics, Vol. 41-4, December 1974.

4. Kelley, J.M., Eidinger, J.M., Derham, C.J., "A Practical Soft-Story Earthquake Isolation System," Earthquake Engineering Research Center, University of California, Report UC/EERC-77/27, November 1977.

5. Kelley, J.M., Skinner, M.S., "The sign of Steel Energy-Absorbing Restrainers and Their Incorporation into Nuclear Power Plants for Enhanced Safety," Volume 4, Earthquake Engineering Research Center, University of California, Report UCB/EERC - 79/10, February 1979.

6. Kaynia, A.M., "Dynamic Stiffness and Seismic Response of Sleeved Piles," Department of Civil Engineering Research Report R80-12, MIT, May 1980.

7. Shyam Sunder, S., "On the Standard Processing of Strong-Motion Earthquake Signals," Department of Civil Engineering Research Report R80-38, MIT, September 1980.

8. Shyam Sunder, S., and Betsy Schumacker, "Earthquake Motions and Response Spectra Using a New Data Processing Technique," to be submitted for publication in the ASCE Journal of Engineering Mechanics.

9. Earthquake Engineering Research Laboratory (EERL), "Strong-Motion Earthquake Accelerograms, Uncorrected Digitized Accelerograms - Printouts and Computer Plots," Vol. 1, EERL, California Institute of Technology, 1975.

10. Brady, A.G., Perez, V., and Mork, P.N., "The Imperial Valley Earthquake, October 15, 1979. Digitization and Processing of Accelerograph Records," Open File Report 80-703, Seismic Engineering Data Report, United States Department of the Interior, Geological Survey, Menlo Park, California, 1980.

11. Trifunac, M.D., and Lee, V.W., "Uniformly Processed Strong Earthquake Ground Accelerations in the Western United States of America for the Period from 1933 to 1971: Corrected Acceleration, Velocity, and Displacement Curves," Report No. 78-01, Department of Civil Engineering, University of Southern California, Los Angeles, CA, 1978.

APPENDIX

Corrected Earthquake Time-Histories

and Response Spectra

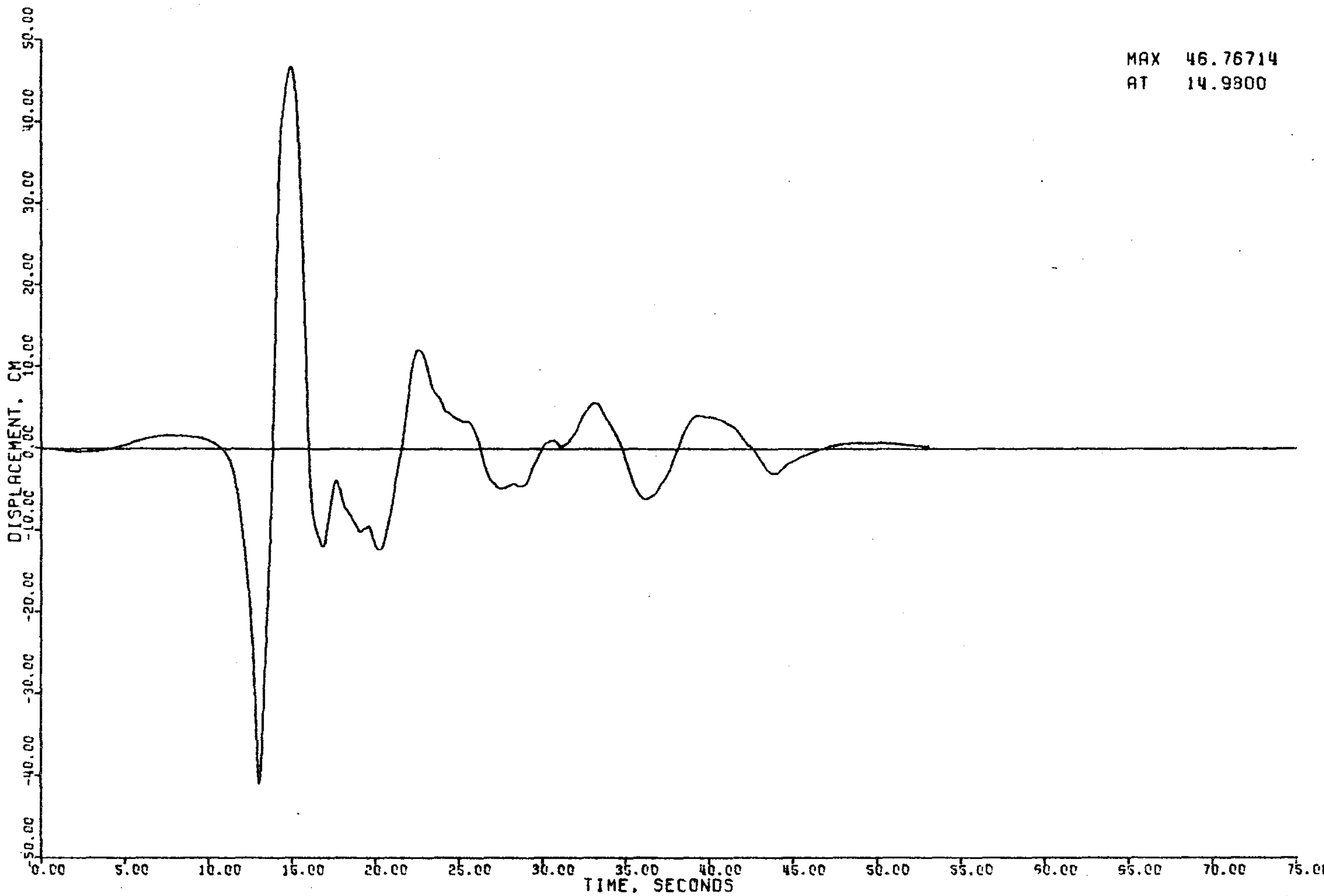

Fig. A.2 IMPERIAL VALLEY EARTHQUAKE - EL CENTRO ARRAY 7 - I V COLLEGE

DATE: OCT. 15, 1979 TIME: 2317 UTC COMPONENT: 230
BPF: 0.049-0.070, 25.0-30.6 HZ

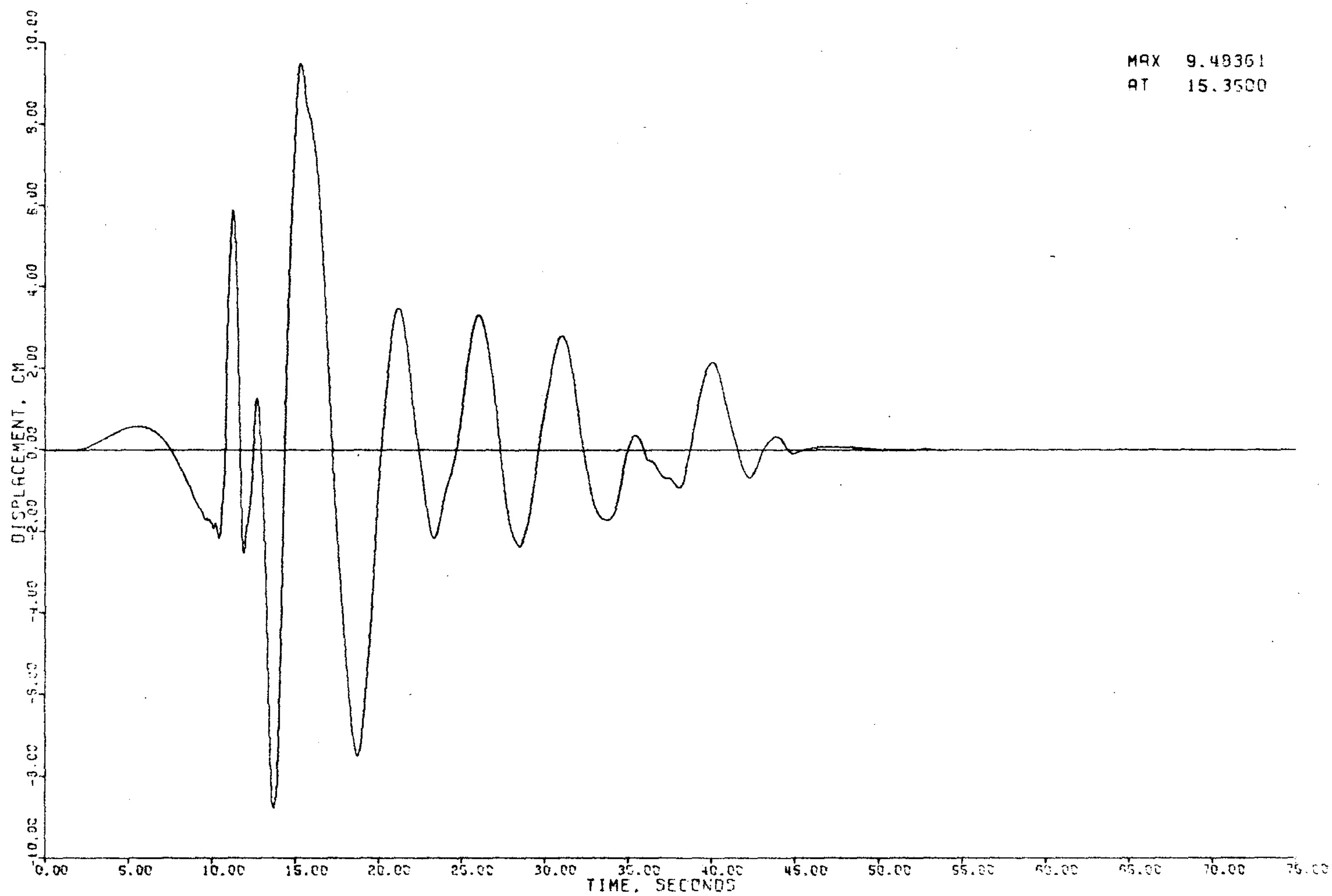

Fig. A.4 IMPERIAL VALLEY EARTHQUAKE - EL CENTRO ARRAY 7 - I V COLLEGE

DATE: OCT. 15, 1979 TIME: 2317 UTC COMPONENT: UP
BPF: 0.048-0.070, 25.0-30.5 HZ

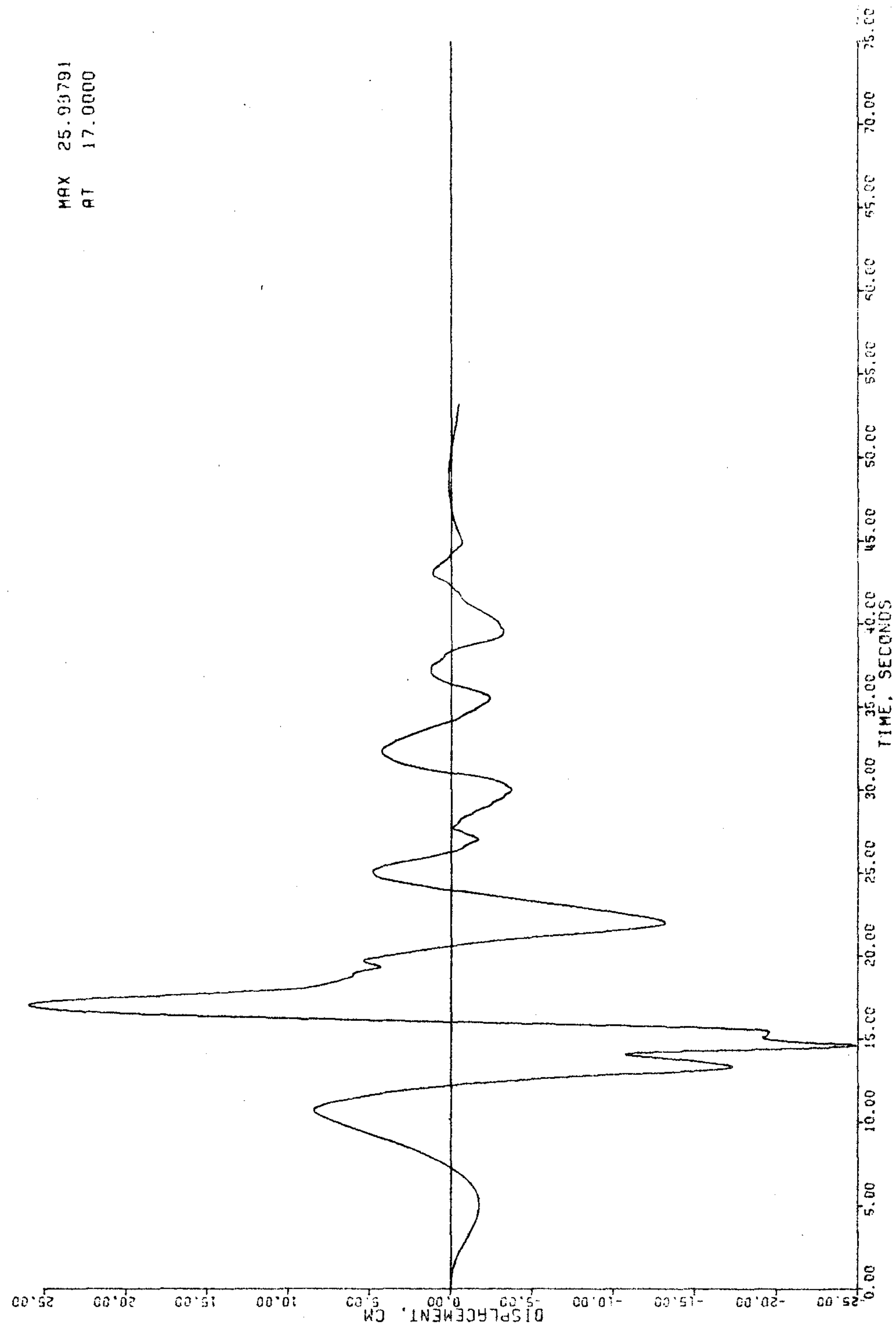

Fig. A.6 IMPERIAL VALLEY EARTHQUAKE - EL CENTRO ARRAY 7 - I V COLLEGE

DATE: OCT. 15, 1979 TIME: 2317 UTC COMPONENT: 140
BPF: 0.048-0.070, 25.0-30.5 HZ

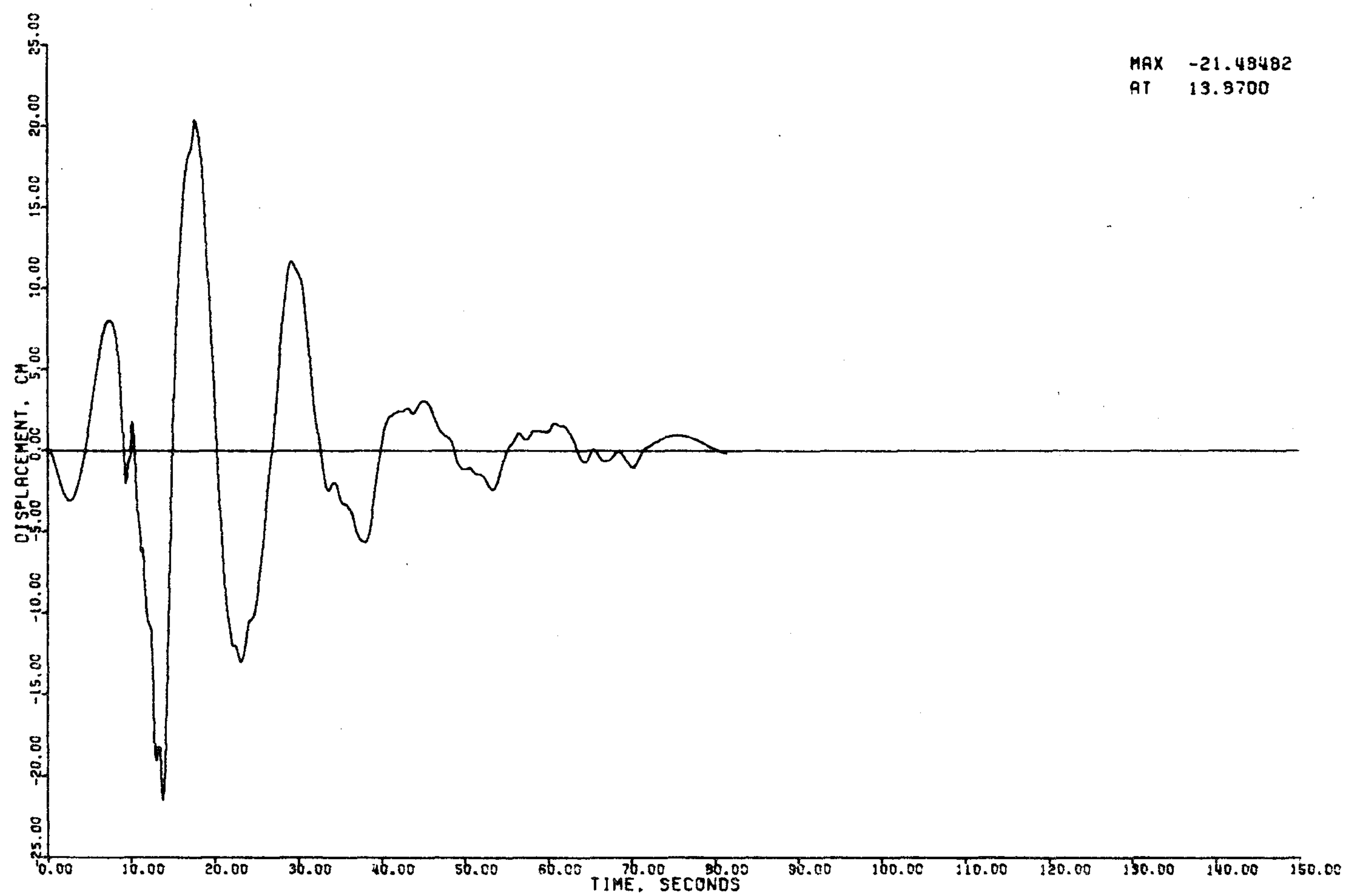

Fig. A.8 LONG BEACH EARTHQUAKE - MIT STANDARD PROCESSING SCHEME

DATE: MARCH 11, 1933 TIME: 1754 PST COMPONENT: SOUTH
BPF: 0.049-0.070, 19.5-24.0 HZ

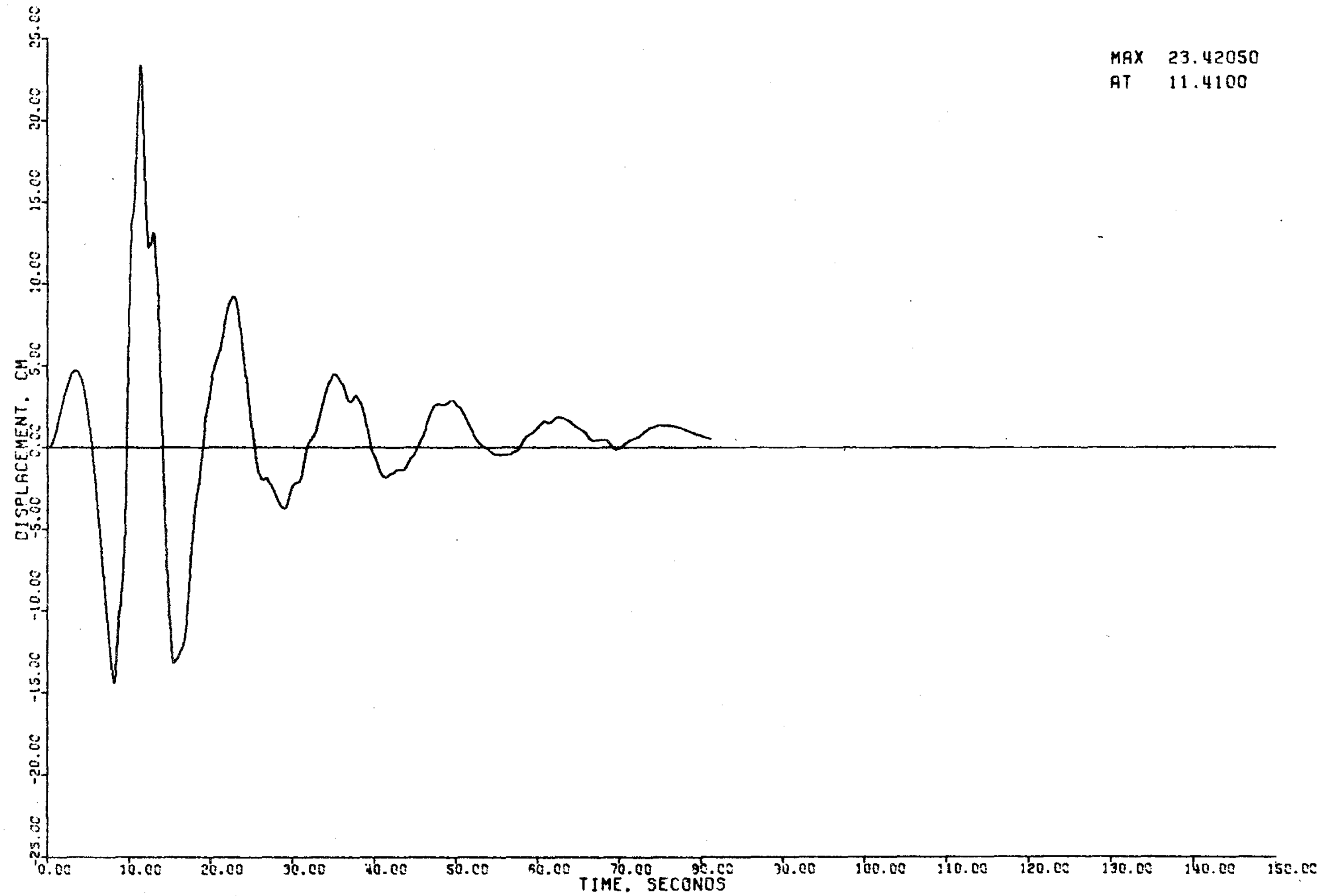

Fig. A.10 LONG BEACH EARTHQUAKE - PUBLIC UTILITIES BLDG

DATE: MAR 10, 1933 TIME: 1754 PST COMPONENT: UP
BPF: 0.056-0.080, 16.0-21.2 HZ

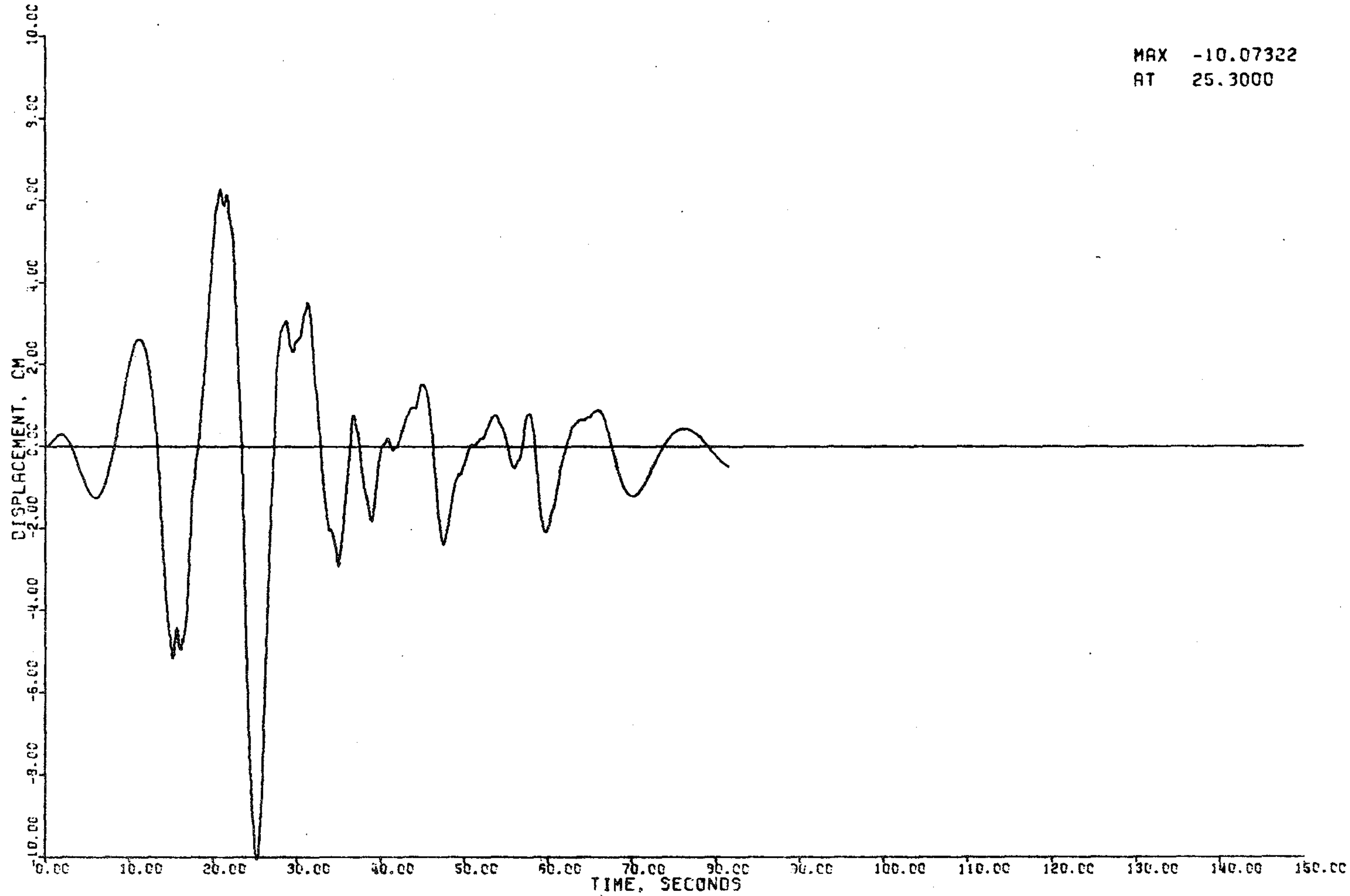

Fig. A.12 SITKA ALASKA EARTHQUAKE - SITKA OBSERVATORY

DATE: JULY 30, 1972 TIME: 2145 GMT COMPONENT: NORTH
BPF: 0.056-0.08C, 25.0-30.6 HZ

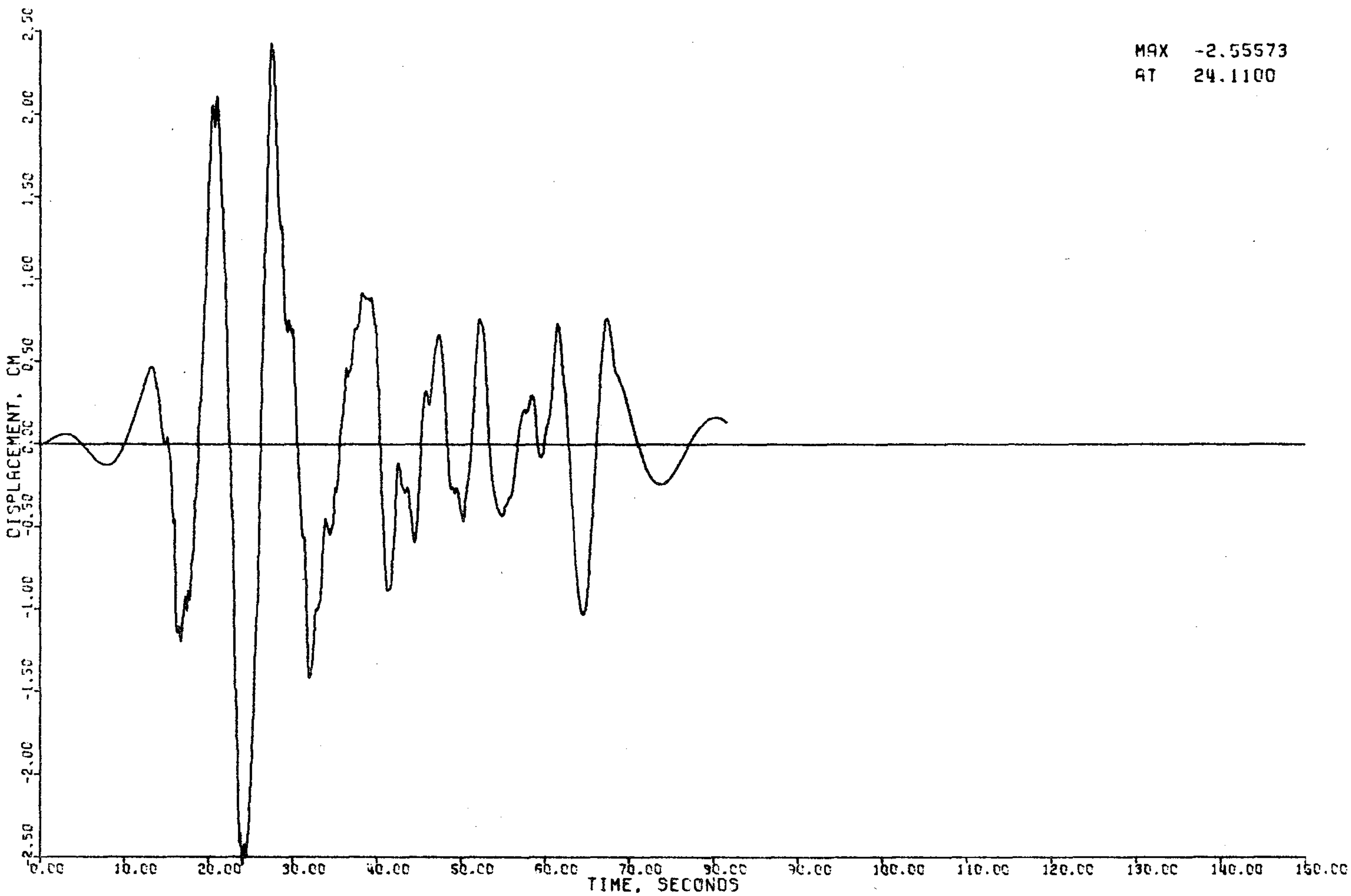

Fig. A.14 SITKA ALASKA EARTHQUAKE - SITKA OBSERVATORY

DATE: JULY 30, 1972 TIME: 2145 GMT COMPONENT: DOWN
BPF: 0.056-0.080, 25.0-30.6 HZ

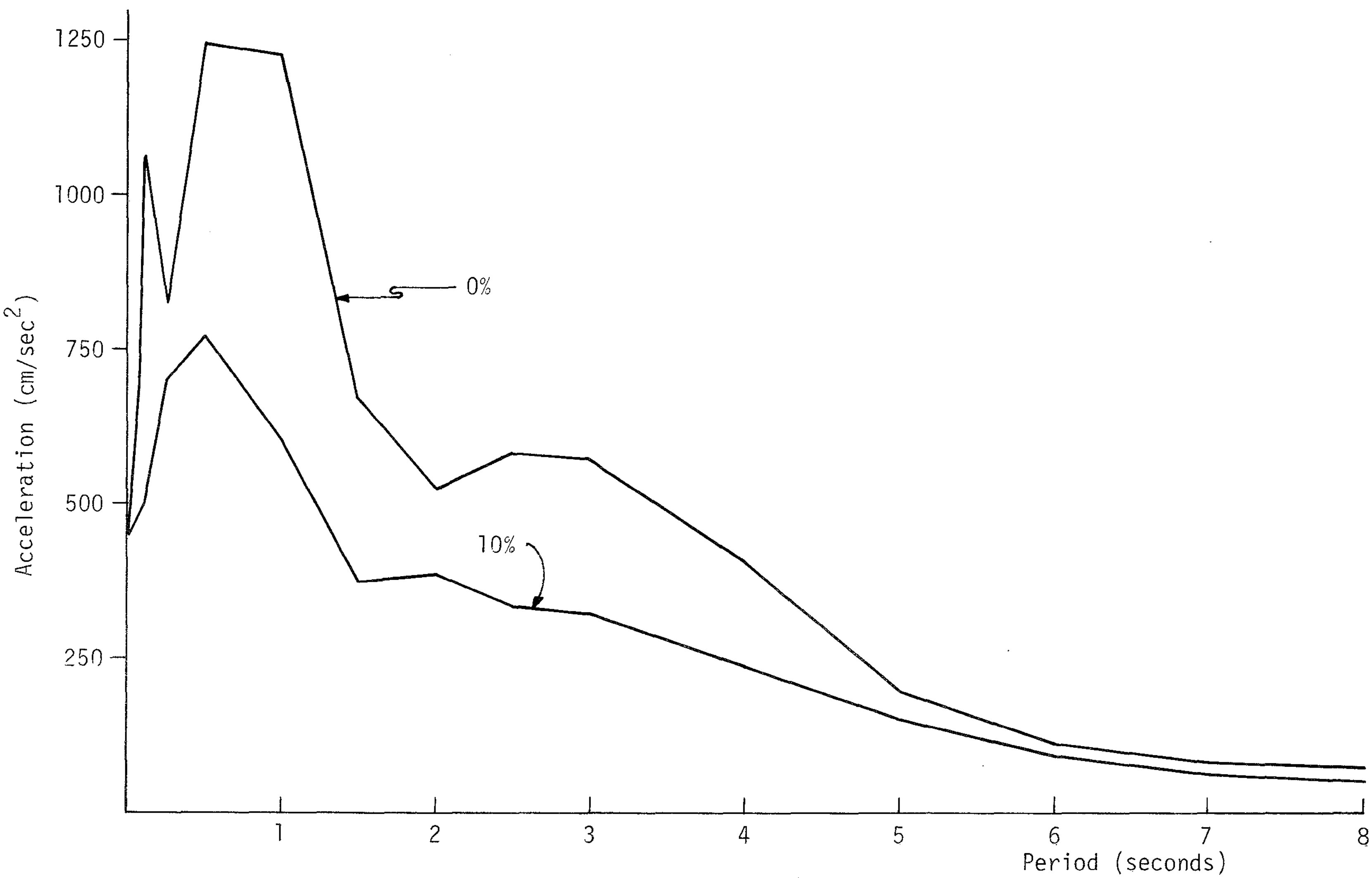

Fig. A.16 Acceleration Response Spectra, EQ-1 (H)

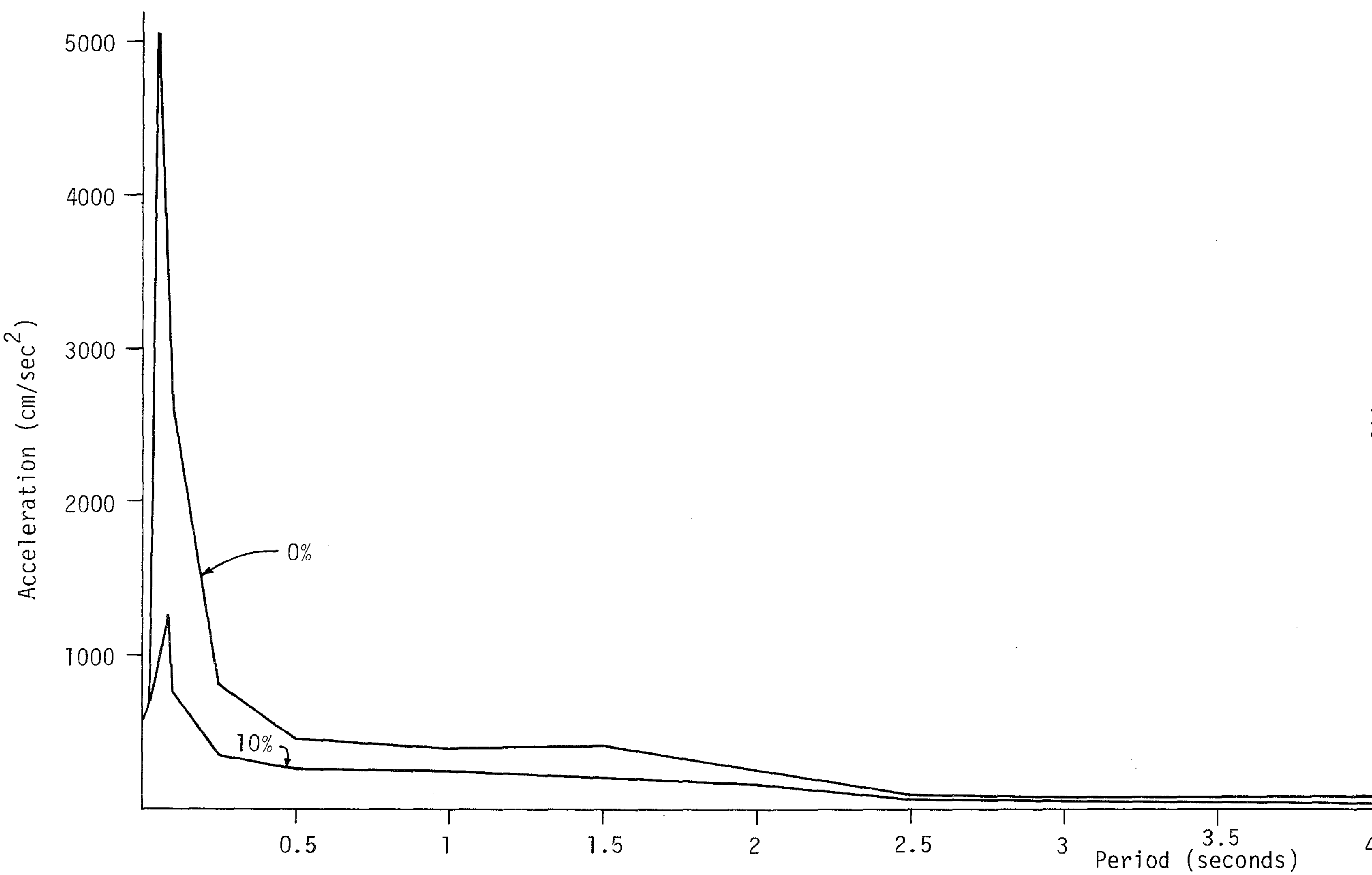

Fig. A.18 Acceleration Response Spectra, EQ-1, EQ-2 (V)

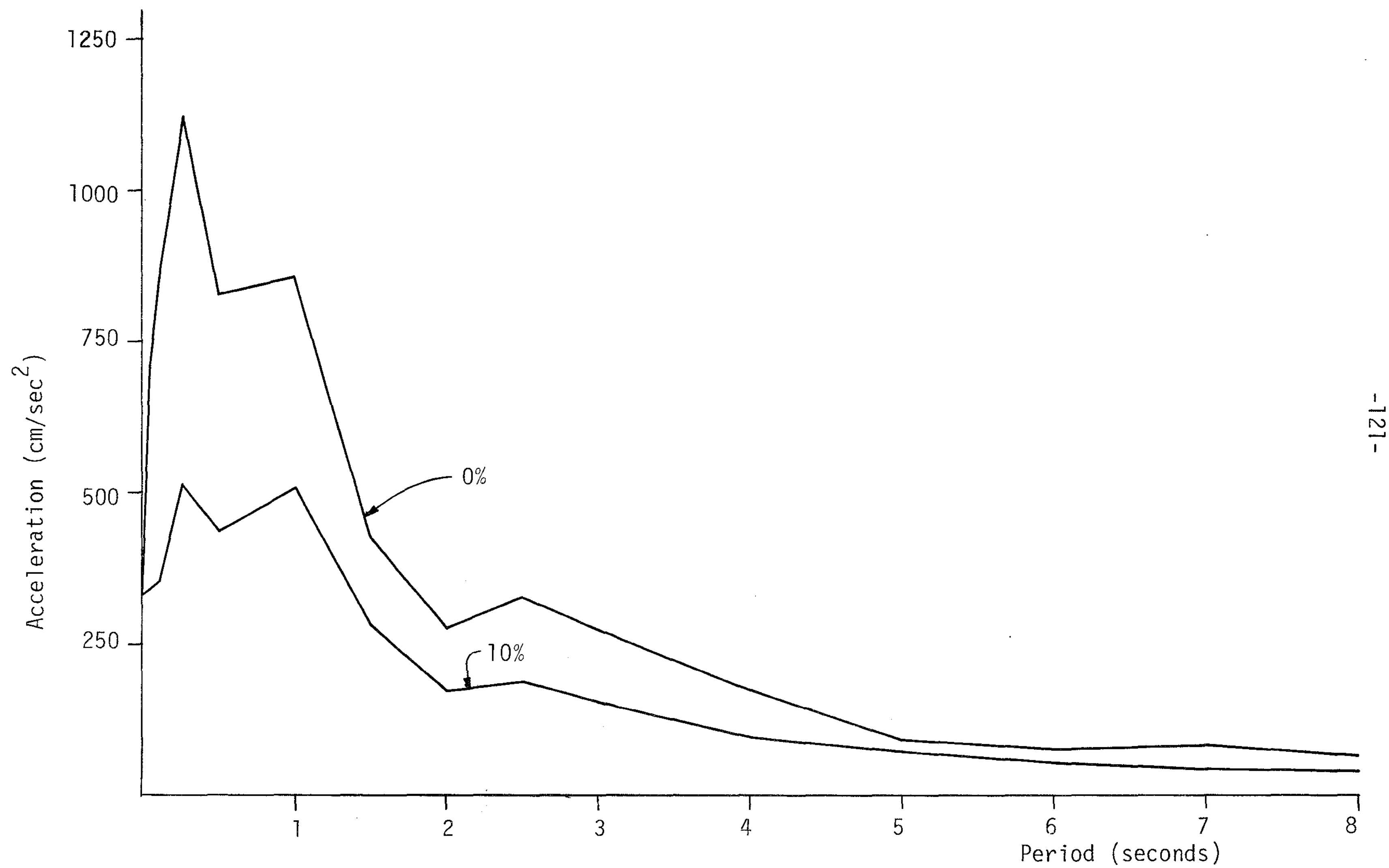

Fig. A.20 Acceleration Response Spectra, EQ-2 (H)

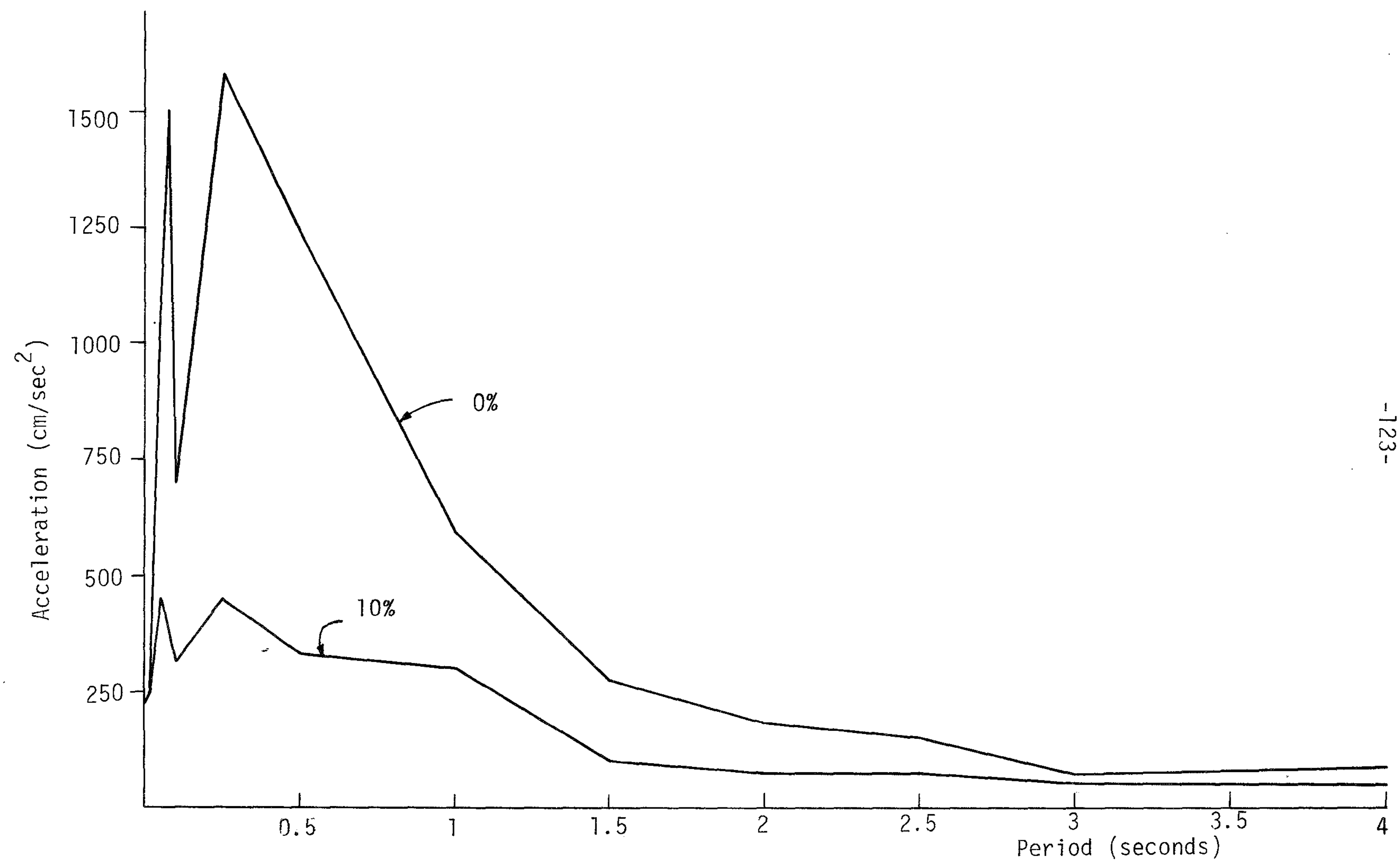

Fig. A.22 Acceleration Response Spectra, EQ-3 (H)

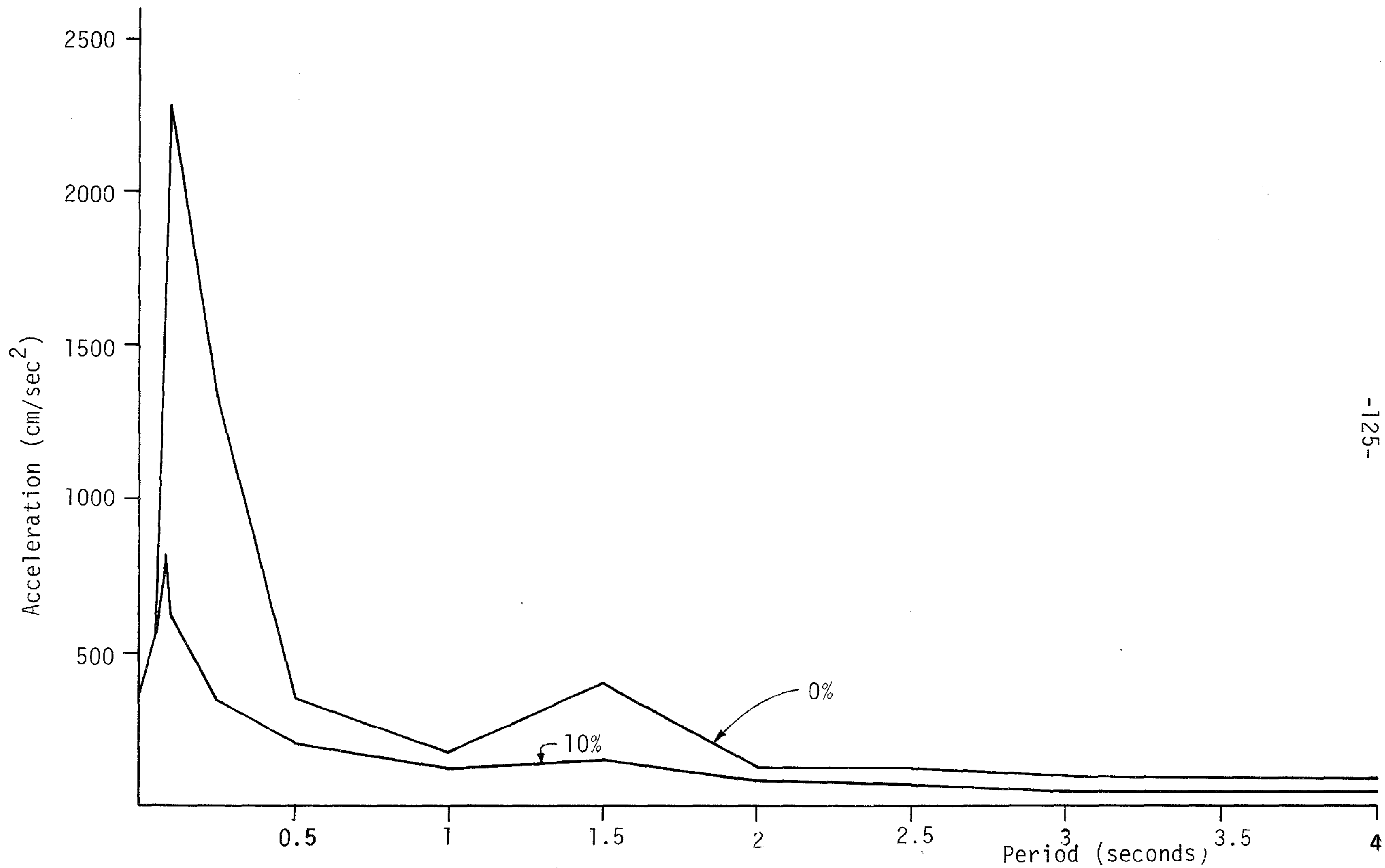

Fig. A.24 Acceleration Response Spectra, EQ-3 (V)

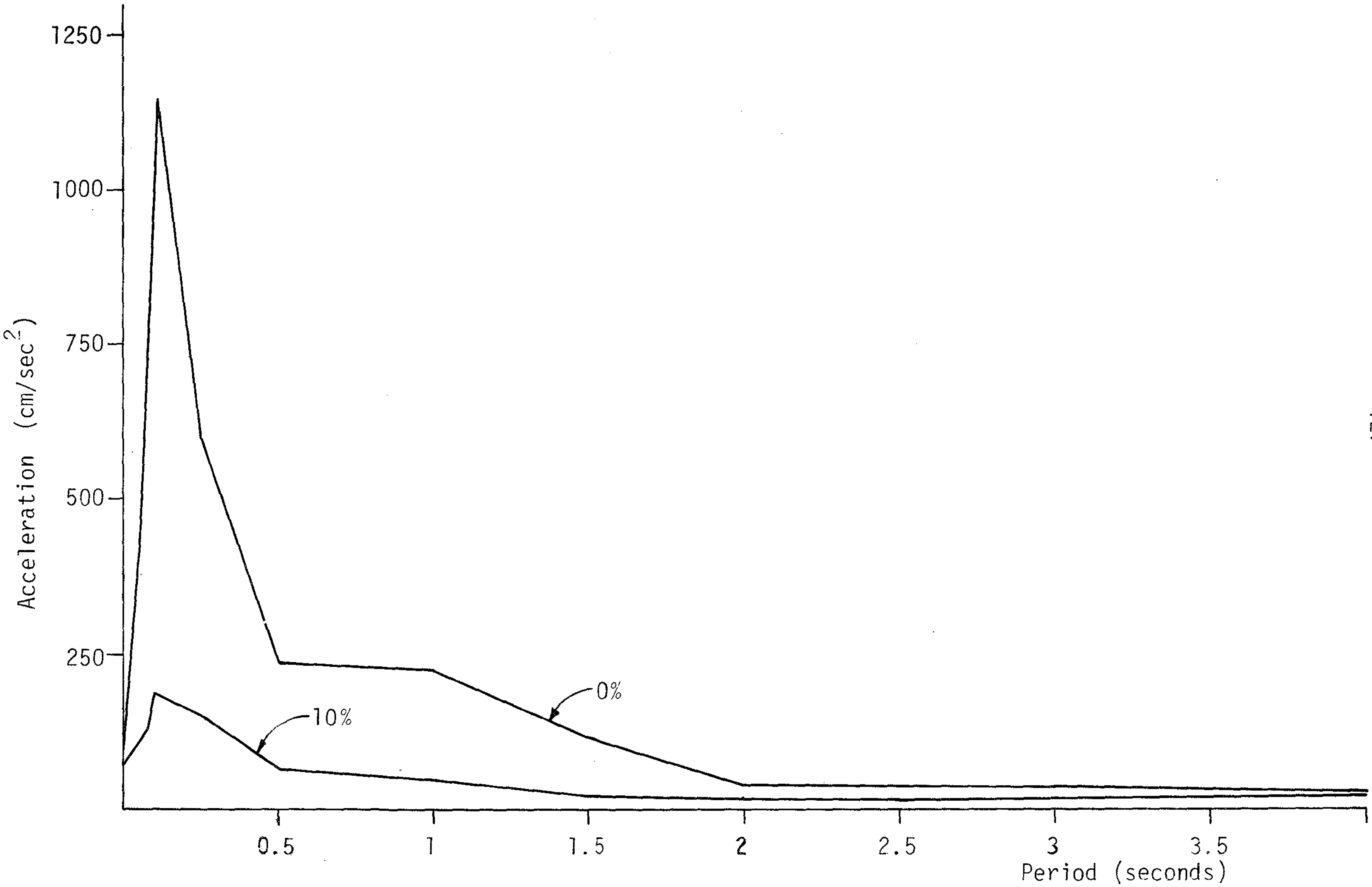

Fig. A.26 Acceleration Response Spectra, EQ-4 (H)

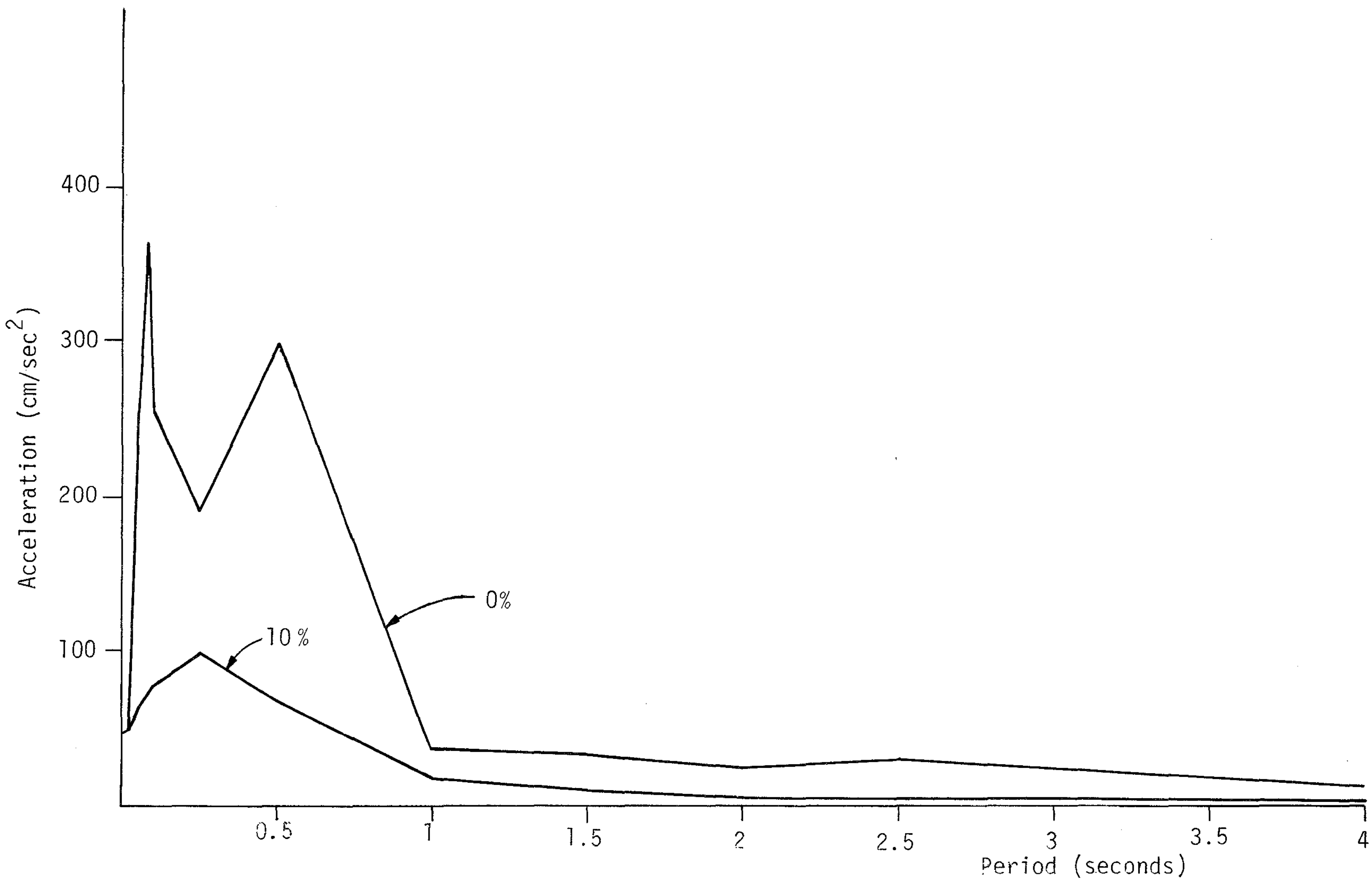

Fig. A.28 Acceleration Response Spectra, EQ-4 (V)